frontiers | Frontiers in Energy Research

TYPE Original Research
PUBLISHED 29 September 2022
DOI 10.3389/fenrg.2022.941705

OPEN ACCESS

EDITED BY
Pallavi Choudekar,
Amity University, India

REVIEWED BY
Essam Halim Houssein,
Minia University, Egypt
Mourad Yessef,
Sidi Mohamed Ben Abdellah University,
Morocco

*CORRESPONDENCE
Fatima Daqaq,
fati.daqaq@gmail.com
Salah Kamel,
skamel@aswu.edu.eg

SPECIALTY SECTION
This article was submitted to Smart Grids, a section of the journal Frontiers in Energy Research

RECEIVED 11 May 2022
ACCEPTED 28 July 2022
PUBLISHED 29 September 2022

CITATION
Daqaq F, Ouassaid M, Kamel S, Ellaia R and El-Naggar MF (2022), A novel chaotic flower pollination algorithm for function optimization and constrained optimal power flow considering renewable energy sources.
Front. Energy Res. 10:941705.
doi: 10.3389/fenrg.2022.941705

A novel chaotic flower pollination algorithm for function optimization and constrained optimal power flow considering renewable energy sources

Fatima Daqaq[1,2]*, Mohammed Ouassaid[2], Salah Kamel[3]*, Rachid Ellaia[1,2] and Mohamed F. El-Naggar[4,5]

[1]Laboratory of Study and Research for Applied Mathematics, Mohammadia School of Engineers, Mohammed V University, Rabat, Morocco, [2]Engineering for Smart and Sustainable Systems Research Center, Mohammadia School of Engineers, Mohammed V University, Rabat, Morocco, [3]Electrical Engineering Department, Faculty of Engineering, Aswan University, Aswan, Egypt, [4]Department of Electrical Engineering, College of Engineering, Prince Sattam Bin Abdulaziz University, Al-Kharj, Saudi Arabia, [5]Department of Electrical Power and Machines Engineering, Faculty of Engineering, Helwan University, Helwan, Egypt

This study presents an improved chaotic flower pollination algorithm (CFPA) with a view to handle the optimal power flow (OPF) problem integrating a hybrid wind and solar power and generate the optimal settings of generator power, bus voltages, shunt reactive power, and tap setting transformers. In spite of the benefits of FPA, it encounters two problems like other evolutionary algorithms: entrapment in local optima and slow convergence speed. Thus, to deal with these drawbacks and enhance the FPA searching accuracy, a hybrid optimization approach CFPA which combines the stochastic algorithm FPA that simulates the flowering plants process with the chaos methodology is applied in this manuscript. Therefore, owing to the various nonlinear constraints in OPF issue, a constraint handling technique named superiority of feasible solutions (SF) is embedded into CFPA. To confirm the performance of the chaotic FPA, a set of different well-known benchmark functions were employed for ten diverse chaotic maps, and then the best map is tested on IEEE 30-bus and IEEE 57-bus test systems incorporating the renewable energy sources (RESs). The obtained results are analyzed statistically using non-parametric Wilcoxon rank-sum test in view of evaluating their significance compared to the outcomes of the state-of-the-art meta-heuristic algorithms such as ant bee colony (ABC), grasshopper optimization algorithm (GOA), and dragonfly algorithm (DA). From this study, it may be established that the suggested CFPA algorithm outperforms its meta-heuristic competitors in most benchmark test cases. Additionally, the experimental results regarding the OPF problem demonstrate that the integration of RESs decreases the total cost by 12.77% and 33.11% for the two systems, respectively. Thus, combining FPA with chaotic sequences is able to accelerate the convergence and provide better accuracy to find optimal solutions. Furthermore, CFPA (especially with the Sinusoidal map) is challenging in solving complex real-world problems.

KEYWORDS

constraint handling technique, flower pollination algorithm, chaotic map, wind-solar system, optimal power flow

1 Introduction

Nature-inspired computation algorithms have been evolved during the last few decades, supplying a varied source of approaches that address diverse fields, such as industrial designs, economics, business activities, engineering, etc. Generally, there are two categories of optimization techniques: stochastic and deterministic algorithms (Vasant, 2012). The deterministic kind of approaches proceed rigorously; they produce an accurate outcome for a given design variable. However, in spite of their fast convergence, they fail to reach the global solution; hence, they get stuck in local optima and fail to deal with derivative-free issues. In contrast, the stochastic algorithms are among the best and effective strategies in finding optimal solutions, conflicting with the classical optimization approaches. This kind of algorithm has been widely utilized due to its capability to obtain global optimum solutions escaping from local optima and its ease of implementation. Some of the well-regarded meta-heuristic algorithms are as follows: Genetic Algorithm (GA), which is the first stochastic algorithm inspired by John Holland in 1960 (Holland, 1975), followed by Simulated Annealing (SA) in 1983 (Kirkpatrick et al., 1983), Particle Swarm Optimization (PSO) in 1995 by Kennedy (Kennedy and Eberhart, 1995), and more approaches that were developed later, such as Ant Bee Colony (ABC) (Basturk and Karaboga, 2006), Arithmetic Optimization Algorithm (AOA) (Abualigah et al., 2021a), Harris Hawks Optimization (HHO) (Heidari et al., 2019), Sin Cosine Algorithm (SCA) (Mirjalili, 2016), Black Widow Optimization (BWO) (Hayyolalam and Pourhaji, 2020), Dynamic differential annealed optimization (DDAO) (Ghafil and Jármai, 2020), Levy Flight Distribution (LFD) (Essam et al., 2020), Salp Swarm Algorithm (SSA) (Mirjalili et al., 2017), Henry Gas Solubility Optimization (HGSO) (Hashim et al., 2019), Manta Ray Foraging Optimization (MRFO) (Zhao et al., 2020), starling murmuration optimizer (SMO) (Zamani et al., 2022), Honey Badger Algorithm (HBA) (Hashim et al., 2022), Reptile Search Algorithm (RSA) (Abualigah et al., 2022), Aquila Optimizer (AO) (Abualigah et al., 2021b), and so on. All these algorithms divide the search process into two important characteristics: exploration and exploitation with a specific probability; these two phases are also called diversification and intensification. The first phase is considered as the essential step in which the algorithm can examine the search space more effectively and generate a new diverse solution as possible with jumping out from any local optima. Meanwhile, the exploitation or intensification phase attempts to use the information of the obtained current best solutions from the exploration or diversification phase (Yang, 2010). In numerous instances, exploitation and exploration are not balanced, and due to the random nature of meta-heuristic algorithms, there is no explicit frontier between these two mechanisms (Mirjalili et al., 2014). Therefore, these issues leave the stochastic approaches stuck in the local optimum without balancing properly between the exploitation and exploration. Moreover, in spite of the benefits of the intelligence algorithms, they require some improvement to satisfy the diverse characteristics of complex real-world applications, which means that no approach is qualified in resolving the diverse kind of optimization problems. In that regard, the No-Free Lunch (NFL) theorem (Wolpert and Macready, 1997) validates this and opens the way for developers to create new approaches and enhance the quality of the existing ones.

Recently, a third group of nature algorithms can be considered, and it is a hybrid between stochastic and deterministic algorithms. The combination of meta-heuristics with conventional methods is a practical remedy to enhance both exploitation and exploration and then to raise the performance of stochastic algorithms, by overcoming the slow convergence drawback, local optima entrapment, and the meta-heuristics random constructions. One of the most known mathematical techniques is combining chaotic sequences with stochastic algorithms. Additionally, the chaos is a random state which can appear in the nonlinear dynamical systems and bounded properties, non-convergent and non-periodic (Alatas, 2010). This chaos can be integrated in the stochastic algorithms with the intention of optimizing their performances. Accordingly, the chaos has been extensively embedded in several evolutionary approaches. In this regard, here are some computation algorithms that have been improved: chaotic firefly algorithm (CFA) (Gandomi et al., 2013), chaotic ant swarm optimization (CASO) (Cai et al., 2007), chaotic genetic algorithm (CGA) (Abdullah et al., 2012), chaotic particle swarm optimization (CPSO) (He et al., 2009), hybridizing chaotic sequences with memetic differential evolution algorithm (Jia et al., 2011), chaotic krill herd algorithm (CKHA) (Wanga et al., 2014), chaotic bio-geography based optimization (CBBO) (Saremi et al., 2014), chaotic artificial immune system algorithm (CAIS) (Jordehi, 2015), chaotic water cycle algorithm

(CWCA) (Heidari et al., 2017), chaotic based big bang-big crunch algorithm (BBBC) (Jordehi, 2014), chaotic manta ray foraging optimization (CMRFO) (Daqaq et al., 2022), chaotic bat algorithm (CBA) (Mugemanyi et al., 2020), chaotic atom search optimization (CAS) (Too and Abdullah, 2020), Coyote Optimization Algorithm (COA) (Tong et al., 2022), etc.

In this current work, the authors focus on the hybridization of chaos maps with a stochastic approach named flower pollination algorithm (FPA), in view of switching between local and global pollination. Instead of random numbers of diverse parameters of FPA, chaotic maps are replaced to not follow the uniform distribution. With regard to the FPA, it has been pointed out in diverse academic fields and real-world applications, especially in science and engineering, that it performs better than other well-known algorithms. From this perspective, the powerful advantages of FPA and its borrowed approaches motivate us to develop a novel version of FPA based on chaos maps in view of solving the OPF incorporating RESs. In that aspect, among these studies that have been published on FPA and its variants, the study by (Singh and Kaur, 2019) selects the optimal features for anomaly detection in networks using the standard flower pollination algorithm. According to the study by (Samy et al., 2019), the authors applied FPA to develop a techno-economic feasibility analysis for an off-grid hybrid renewable energy system. In the study by (Priya and Rajasekar, 2019), PEMFC modeling has been successfully tackled by using FPA. A recent study (Wang et al., 2019a) presented FPA with the wireless sensor networks to deploy heterogeneous node radiation. In another research work (Wang et al., 2019b), a discrete flower pollination algorithm–based multi-objective optimization is investigated to solve the stochastic two-sided partial disassembly line. A hybridization of FPA with wind-driven optimization is adopted in the study by (Niu et al., 2019) in order to develop the global and local pollination processes. (Rodrigues et al., 2020) suggested an adaptive flower pollination algorithm that can dynamically modify its parameter. (Shambour et al., 2019) employed the direct search method in the global pollination process to improve the convergence and accuracy of the original FPA. For more information concerning the FPA and its variants, refer to the recent review (Abdel-Basset and Shawky, 2019). In relation to the previously published work and in an attempt to prove the FPA superiority, the proposed approach is validated and tested on thirteen benchmark test problems. In addition to these test suites, a real-world problem under the name of optimal power flow (OPF) is applied to affirm the capability and effectiveness of this novel algorithm in solving real complex functions.

The OPF has played an important task in the planning and operation of power systems over recent decades (Bonab et al., 2016). Furthermore, the optimal power flow problem is characterized as a non-convex, nonlinear, large-scale, and highly constrained optimization problem (Vaccaro and Cañizares, 2018), and the main key of the OPF issue is to diminish some objectives such as fuel cost, emission, voltage deviation, and power loss by decreasing the control variable values with respect to the different constraints such as equal and inequal limitations. Moreover, the optimal power flow issue, including renewable energy, has taken up increasing attention in many research studies owing to the environmental benefits and low operation cost. Besides, the renewable resources used most in the world are solar and wind power. On this basis, this current work formulates and solves the OPF problem with and without merging a hybrid wind-photovoltaic energy into 30-bus and 57-bus systems. In that aspect, the renewable sources are installed instead of some conventional generators. Accordingly, an extensive number of meta-heuristic algorithms have been undertaken to deal with the OPF problem. Some recently introduced approaches that have been efficiently applied in this field can be found in these references (Abaci and Yamacli, 2016; Bouchekara et al., 2016a; Bouchekara et al., 2016b; Bouchekara et al., 2016c; Chaib et al., 2016; Trivedi et al., 2016; Bentouati et al., 2017; Duman, 2017; Mohamed et al., 2017; Yuan et al., 2017; Biswas et al., 2018a; Biswas et al., 2018b; El-Fergany and Hasanien, 2018; Morshed et al., 2018; Taher et al., 2019a; Taher et al., 2019b; El-Sattar et al., 2019; Elattar, 2019; Nguyen, 2019; Shilaja and Arunprasath, 2019; Alhejji et al., 2020; Warid, 2020; Alasali et al., 2021; Daqaq et al., 2021; Meng et al., 2021; Sulaiman et al., 2021; Yessef et al., 2022a; Yessef et al., 2022b; Houssein et al., 2022).

Experimental results display that the proposed chaotic FPA outstrips the basic FPA and some re-implemented algorithms such as ant bee colony (ABC), grasshopper optimization algorithm (GOA), dragonfly algorithm (DA), and even the existing well-known algorithms reported in the literature.

The major features of this research study can be listed as follows:

- A novel hybridization method based on FPA and chaos sequences is proposed.
- Ten chaotic maps widely used in the literature are integrated.
- A constraint handling method has been merged in CFPA, named superiority of feasible solutions (SF).
- Thirteen benchmark problems are implemented to show the performance of CFPA.
- The best chaotic map is applied to OPF with thermal, wind, and solar power.
- Some evaluation measures are utilized, such as mean, max, min fitness, standard deviation, and statistical Wilcoxon test.
- The proposed algorithm is compared with basic FPA and other stochastic methods.

The rest of the manuscript is arranged as follows: Section 2 gives a brief introduction of the standard FPA, its chaotic variant CFPA-based SF strategy, and a description of the ten chaos maps' functions. Section 3 introduces the wind, solar, and OPF models. The findings and discussions are investigated in Section 4. Finally, in Section 5, the article ends with a conclusion.

2 Problem methodology

2.1 Renewable energy model

Nowadays, the treatment of renewable energy resources (RESs) in power systems is developing rapidly, especially wind and PV power. The RESs contribute in decreasing CO_2 emissions and enhancing the quality and reliability of the power system. Solar irradiance and wind distribution are modeled using the Lognormal and Weibull probability density function, respectively (Biswas et al., 2017). Lognormal fitting of solar irradiance, Weibull fitting of wind speed, and frequency distribution are generated after 8,000 runs of Monte Carlo simulation, as depicted in Figures 1, 2 (Xie et al., 2018). The associated cost of each of these resources consists of three terms: the direct cost, penalty cost, and reserve cost (Biswas et al., 2017). Table 1 tabulates the parameters of the considered systems. Table 2 provides the cost and emission coefficients for the thermal generators of IEEE 30-bus and 57-bus test systems. All parameters of the solar and the wind are described in detail in Table 3.

2.1.1 Wind power

For modeling the variability of wind flow, a Weibull probability distribution function is applied (Chang, 2010):

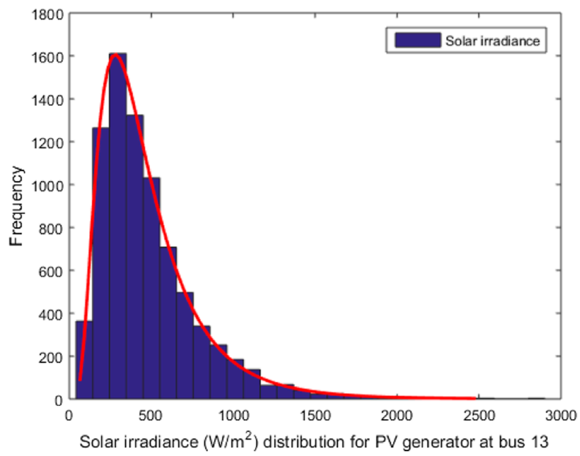

FIGURE 2
Distribution of solar irradiance for the solar generator at the 13^{th} buses.

$$f(v) = \left(\frac{k}{c}\right)\left(\frac{v}{c}\right)^{(k-1)} \exp\left[-\left(\frac{v}{c}\right)^{k}\right], \quad v \geq 0 \tag{1}$$

where k and c represent the shape and scale factors of Weibull distribution, respectively.

The wind generator's output power can be defined using the stochastic wind speed as follows (Chang, 2010):

$$p_w(v) = \begin{cases} 0 & v < v_{\text{in}} \text{ and } v > v_{\text{out}} \\ p_{wr}\left(\dfrac{v - v_{\text{in}}}{v_r - v_{\text{in}}}\right) & v_{\text{in}} \leq v \leq v_r \\ p_{wr} & v_r < v \leq v_{\text{out}} \end{cases} \tag{2}$$

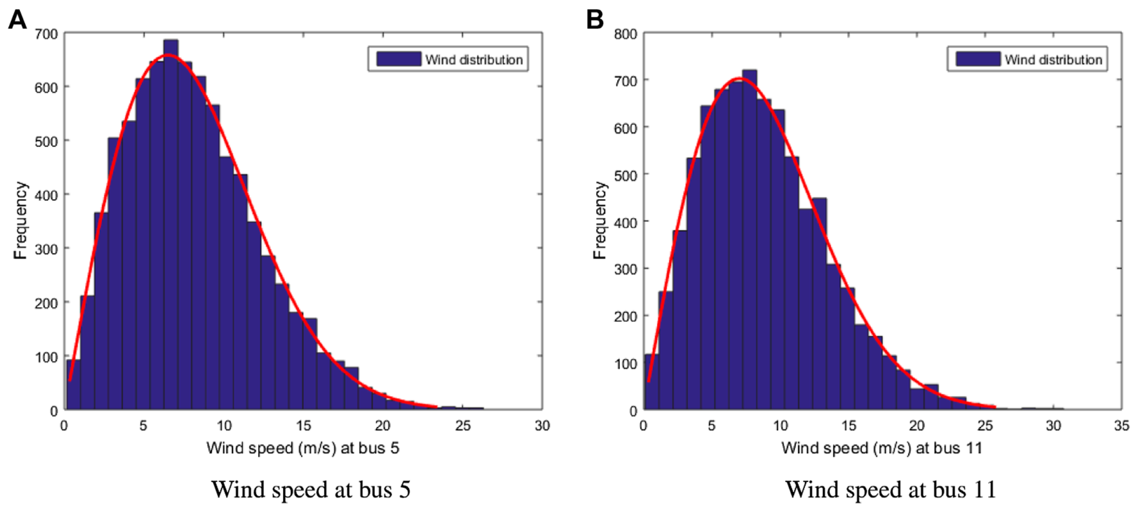

FIGURE 1
Distribution of wind speed for wind generators. **(A)** Wind speed at bus 5 and **(B)** wind speed at bus 11.

TABLE 1 Characteristics of the systems.

Systems Characteristics	30-bus IEEE 30-bus test system data, (1961) Value	Details	57-bus IEEE 57-bus test system data, (1960) Value	Details
Buses	30	-	57	-
Branches	41	-	80	-
Generators	3	Buses: 1, 2, and 8	4	Buses: 1, 3, 8, and 12
Slack bus	1	Buses: 1	1	Buses: 1
Wind generators	2	Buses: 5 and 11	2	Buses: 2 and 6
Solar generators	1	Buses: 13	1	Buses: 9
Shunts	9	Buses: 10, 12, 15, 17, 20, 21, 23, 24, and 29	3	Buses: 18, 25, and 53
Transformers	4	Branches: 11, 12, 15, and 36	17	Branches: 19, 20, 31, 35, 36 37, 41, 46, 54, 58, 59, 65, 66 71, 73, 76, and 13
Control variables	24	-	33	-

TABLE 2 Cost and emission coefficients of thermal generators.

	Generator	Bus	a	b	c	d	e	α	β	γ	ξ	λ
IEEE-30	P_{g1}	1	0	2	0.00375	18	0.037	0.04091	−0.05554	0.06490	0.0002	2.857
	P_{g2}	2	0	1.75	0.0175	16	0.038	0.02543	−0.06047	0.05638	0.0005	3.333
	P_{g3}	8	0	3.25	0.00834	12	0.045	0.05326	−0.03550	0.03380	0.002	2
IEEE-57	P_{g1}	1	0	20	0.0775795	18	0.037	0.04091	−0.05554	0.06490	0.0002	0.2857
	P_{g2}	3	0	20	0.25	13.5	0.041	0.06131	−0.05555	0.05151	0.00001	0.6667
	P_{g3}	8	0	20	0.0222222	14	0.040	0.04258	−0.05094	0.04586	0.000001	0.8000
	P_{g4}	12	0	20	0.0322581	12	0.045	0.05326	−0.03555	0.03380	0.0020	0.2000

TABLE 3 Characteristic details of wind-PV generators.

	Wind power				PV power		
Test systems	Wind	Number of turbines	Pwr (MW)	Parameters of Weibull PDF	Solar	Psr (MW)	Parameters of Lognormal PDF
IEEE-30	1 (bus 5)	25	75	k = 2, c = 9	(bus 13)	50	$\mu = 6, \sigma = 0.6$
	2 (bus 11)	20	60	k = 2, c = 10			
IEEE-57	1 (bus 2)	50	150	k = 2, c = 10	(bus 9)	50	$\mu = 6, \sigma = 0.6$
	2 (bus 6)	40	120	k = 2, c = 10			

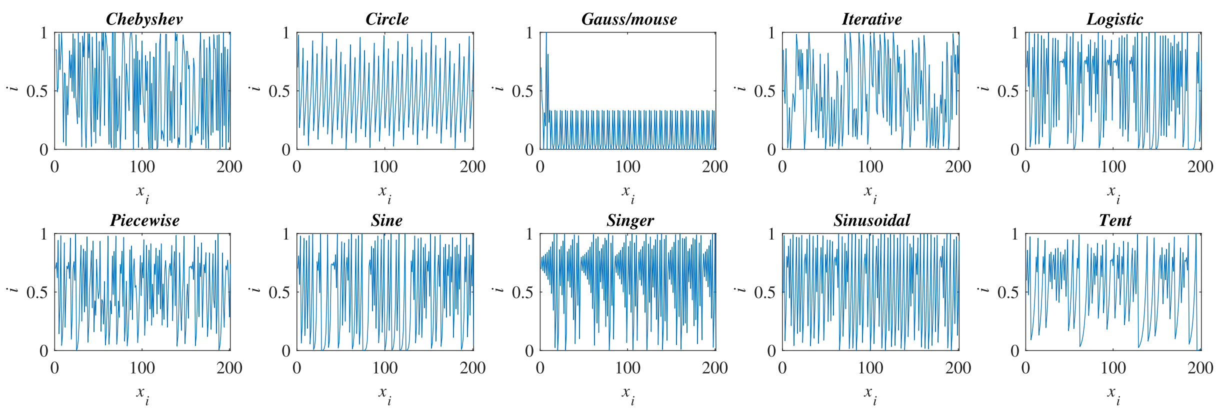

FIGURE 3
Visualization of chaotic maps.

TABLE 4 Chaotic sequences.

	Names	Mathematical formulations	Bounds
CFPA1	Chebyshev	$x_{i+1} = \cos\left(i\cos^{-1}(x_i)\right)$	(-1,1)
CFPA2	Circle	$x_{i+1} = mod\left(x_i + b - \left(\frac{a}{2\pi}\right)\sin\left(2\pi x_i\right), 1\right), \quad a = 0.5 \quad and \quad b = 0.2$	(0,1)
CFPA3	Gausse/mouse	$x_{i+1} = \begin{cases} 1 & x_i = 0 \\ \frac{1}{\mathrm{mod}\,(x_i,1)} & \text{otherwise} \end{cases}$	(0,1)
CFPA4	Iterative	$x_{i+1} = \sin\left(\frac{a\pi}{x_i}\right), \quad a = 0.7$	(-1,1)
CFPA5	Logistic	$x_{i+1} = ax_i\left(1 - x_i\right), \quad a = 4$	(0,1)
CFPA6	Piecewise	$x_{i+1} = \begin{cases} \frac{x_i}{P} & 0 \le x_i \prec P \\ \frac{x_i - P}{0.5 - P} & P \le x_i \prec 0.5 \\ \frac{1 - P - x_i}{0.5 - P} & 0.5 \le x_i < 1 - P \\ \frac{1 - x_i}{P} & 1 - P \le x_i \prec 1 \end{cases}$	(0,1)
CFPA7	Sine	$x_{i+1} = \frac{a}{4}\sin\left(\pi x_i\right), \quad a = 4$	(0,1)
CFPA8	Singer	$x_{i+1} = \mu\left(7.86x_i - 23.31x_i^2 + 28.75x_i^3 - 13.302875x_i^4\right), \quad \mu = 1.07$	(0,1)
CFPA9	Sinusoidal	$x_{i+1} = ax_i^2\sin\left(\pi x_i\right), \quad a = 2.3$	(0,1)
CFPA10	Tent	$x_{i+1} = \begin{cases} \frac{x_i}{0.7} & x_i \prec 0 \\ \frac{10}{3}\left(1 - x_i\right) & x_i \ge 0.7 \end{cases}$	(0,1)

TABLE 5 Benchmark functions.

No	Names	Functions	Type	D	Bounds
F1	Sphere	$f(x) = \sum_{i=1}^{n} x_i^2$	U,S	30	[-100, 100]
F2	Schwefel 2.22	$f(x) = \sum_{i=1}^{n} \lvert x_i \rvert - \prod_{i=1}^{n} \lvert x_i \rvert$	U,N	30	[-10, 10]
F3	Schwefel 1.2	$f(x) = \sum_{i=1}^{n} \left(\sum_{j-1}^{i} x_j\right)^2$	U,N	30	[-100, 100]
F4	Schwefel 2.21	$f(x) = \max\left(\lvert x_i \rvert, l \le i \le n\right)$	U,S	30	[-100, 100]
F5	Rosenbrock	$f(x) = \sum_{i=1}^{n-1} \left[100(x_{i+1} - x_i^2)^2 + (x_i - 1)^2\right]$	U,N	30	[-2.048, 2.048]
F6	Step	$f(x) = \sum_{i=1}^{n} \left([x_i + 0.5]\right)^2$	U,S	30	[-100, 100]
F7	Quartic	$f(x) = \sum_{i=1}^{n} ix_i^4 + \mathrm{rand}(0, 1)$	U,S	30	[-1.28, 1.28]
F8	Schwefel 2.26	$f(x) = \sum_{i=1}^{n} -x_i \sin(\sqrt{\lvert x_i \rvert})$	U,S	30	[-65.536, 65.536]
F9	Rastrigin	$f(x) = \sum_{i=1}^{n} \left(x_i^2 - 10\cos\left(2\pi x_i\right) + 10\right)$	M,S	30	[-100, 100]
F10	Ackley	$f(x) = -20\exp\left(-0.2\sqrt{\frac{1}{n}\sum_{i=1}^{n} x_i^2}\right) - \exp\left(\frac{1}{n}\sum_{i=1}^{n}\cos\left(2\pi x_i\right)\right) + 20 + e$	M,N	30	[-32, 32]
F11	Griewank	$f(x) = \frac{1}{4000}\sum_{i=1}^{n} x_i^2 - \prod_{i=1}^{n}\cos\left(\frac{x_i}{\sqrt{i}}\right) + 1$	M,N	30	[-600, 600]
F12	Penalty 1	$f(x) = \frac{\pi}{n}\left\{10\sin\left(\pi y_1\right) + \sum_{i=1}^{n-1}(y_i - 1)^2\left[1 + \sin^2\left(\pi y_{i+1}\right)\right] + \left(y_n - 1\right)^2\right\} + \sum_{i=1}^{n} u\left(x_i, 10, 100, 4\right)$ $y_i = 1 + \frac{x_i + 1}{4}$ $u\left(x_i, a, k, m\right) = \begin{cases} k(x_i - a)^m & \mathrm{x}_i > a \\ 0 & -a < \mathrm{x}_i < a \\ k(-x_i - a)^m & \mathrm{x}_i < a \end{cases}$	M,N	30	[-50, 50]
F13	Penalty 2	$f(x) = 0.1\left\{\sin^2\left(3\pi x_1\right) + \sum_{i=1}^{n}(x_i - 1)^2\left[1 + \sin^2\left(3\pi x_i + 1\right)\right] + (x_n - 1)^2\left[1 + \sin^2\left(2\pi x_n\right)\right]\right\} + \sum_{i=1}^{n} u\left(x_i, 5, 100, 4\right)$ $u\left(x_i, a, k, m\right) = \begin{cases} k(x_i - a)^m & \mathrm{x}_i > a \\ 0 & -a < \mathrm{x}_i < a \\ k(-x_i - a)^m & \mathrm{x}_i < a \end{cases}$	M,N	30	[-50, 50]

where v_{out}, v_{in}, v_r, v, and p_{wr} are cut-out wind speed, cut-in wind speed, rated wind speed, actual wind speed, and rated output power, respectively.

The total cost of wind energy consists of direct cost associated with scheduled power, penalty cost of underestimation, and reserve cost for overestimation (Biswas et al., 2017), as represented below:

$$C_{Tw,iw} = C_{dw,iw} + C_{uew,iw} + C_{oew,iw} \tag{3}$$

with

$$C_{dw,i} = d_{w,i} P_{ws,i} \tag{4}$$

TABLE 6 Findings of CFPA9 vs. FPA for benchmark functions.

F1	**Min**	**Mean**	**Max**	**SD**	***p*_value**	**F2**	**Min**	**Mean**	**Max**	**SD**	***p*_value**
FPA	987.7615	1813.9519	3076.6316	545.043	3.0199e-11	FPA	21.3294	28.7538	38.265	4.2938	3.0199e-11
CFPA1	18.8979	37.8227	70.6619	12.4083	3.0199e-11	CFPA1	6.1936	10.4859	19.1768	3.5008	3.0199e-11
CFPA2	15.2688	43.1387	88.8292	18.6365	3.0199e-11	CFPA2	6.7896	11.1042	16.0422	2.4499	3.0199e-11
CFPA3	1258.4533	2661.0104	4567.0668	710.4051	3.0199e-11	CFPA3	61.5172	148.965	755.6519	144.622	3.0199e-11
CFPA4	15.0316	38.5099	76.3622	14.8528	3.0199e-11	CFPA4	4.9912	12.1014	24.394	4.7077	3.0199e-11
CFPA5	23.1757	43.8091	72.9427	15.1079	3.0199e-11	CFPA5	4.7404	9.9657	24.8079	3.8124	3.0199e-11
CFPA6	11.0005	23.7962	52.5251	9.1254	3.0199e-11	CFPA6	4.4785	7.5265	14.6163	2.1619	3.0199e-11
CFPA7	27.3814	59.4427	106.8978	18.9277	3.0199e-11	CFPA7	5.7318	12.1761	21.7348	4.0836	3.0199e-11
CFPA8	4.6289	12.1613	24.4056	4.7231	7.3891e-11	CFPA8	2.6943	4.4985	7.6511	1.0836	4.9752e-11
CFPA9	1.0647	2.9895	8.2161	1.6148	N/A	CFPA9	0.9667	1.8497	3.5175	0.54024	N/A
CFPA10	10.8239	26.8769	47.5537	8.8553	3.0199e-11	CFPA10	4.0099	7.9738	15.6067	2.3742	3.0199e-11
F3	Min	Mean	Max	SD	p_value	F4	Min	Mean	Max	SD	P_value
FPA	817.5153	1426.5649	2128.5952	384.2886	3.0199e-11	FPA	15.2297	23.9169	30.718	3.7871	3.0199e-11
CFPA1	210.0864	500.6509	812.7857	139.1303	9.9186e-11	CFPA1	12.0775	15.5532	19.1873	2.292	3.0199e-11
CFPA2	61.4608	173.2704	429.5542	69.5031	0.6735	CFPA2	8.5739	11.7783	15.0979	1.5906	1.1023e-08
CFPA3	1736.9821	2949.5291	4049.0219	732.418	3.0199e-11	CFPA3	24.3423	30.104	36.2199	3.151	3.0199e-11
CFPA4	185.6065	338.6332	547.2509	90.9088	1.8567e-09	CFPA4	9.5883	12.9835	18.1114	1.8006	2.8716e-10
CFPA5	224.7663	549.3806	889.2149	170.4986	7.3891e-11	CFPA5	10.5032	15.537	19.34	2.0655	4.5043e-11
CFPA6	85.2148	223.806	652.1387	120.0867	0.036439	CFPA6	7.7718	11.5285	17.3048	2.0679	7.5991e-07
CFPA7	215.594	569.3826	1097.0103	204.3891	7.3891e-11	CFPA7	12.9187	16.4057	22.3479	2.2246	3.0199e-11
CFPA8	259.8553	486.0341	867.1772	144.4948	7.3891e-11	CFPA8	10.4875	14.2149	19.8762	2.2857	7.3891e-11
CFPA9	54.605	164.8643	406.3104	72.719	N/A	CFPA9	5.9426	8.6958	12.0491	1.4307	N/A
CFPA10	62.9848	245.3469	499.73	95.7697	0.00037704	CFPA10	8.9852	11.4911	14.1238	1.3772	1.85e-08
F5	Min	Mean	Max	SD	P_value	F6	Min	Mean	Max	SD	P_value
FPA	78.4035	127.0658	168.1878	24.3275	3.0199e-11	FPA	1104.3457	1904.3965	3029.3486	490.8553	3.0199e-11
CFPA1	29.9156	34.9191	39.3811	2.3696	3.6897e-11	CFPA1	20.9924	39.089	73.4933	11.4795	3.0199e-11
CFPA2	28.8628	33.1424	43.6933	2.6705	3.6897e-11	CFPA2	16.7506	39.5676	72.1516	14.5482	3.0199e-11
CFPA3	76.0367	166.6979	289.1476	498287	3.0199e-11	CFPA3	1288.717	2781.523	4386.024	905.969	3.0199e-11
CFPA4	29.1252	32.8262	38.4111	1.9846	4.0772e-11	CFPA4	18.9928	38.8026	72.1817	13.9181	3.0199e-11
CFPA5	30.7926	34.384	37.5103	1.7939	3.0199e-11	CFPA5	18.1488	48.2489	119.7437	20.2277	3.0199e-11
CFPA6	29.4226	31.4961	33.9494	1.1896	4.0772e-11	CFPA6	12.2911	31.1671	62.3194	13.2006	3.0199e-11
CFPA7	32.026	36.1206	49.9884	4.0035	3.0199e-11	CFPA7	23.1488	58.2114	87.3031	17.5175	3.0199e-11
CFPA8	28.1309	29.9648	32.6632	1.0156	1.6947e-9	CFPA8	5.9684	12.2077	18.1556	3.7633	9.9186e-11
CFPA9	26.5194	28.1439	30.0759	0.70781	N/A	CFPA9	1.3985	3.9986	9.0732	2.0616	N/A
CFPA10	28.7147	31.7536	39.2258	2.2741	1.2057e-10	CFPA10	5.5157	25.5495	88.5343	15.5952	5.4941e-11
F7	Min	Mean	Max	SD	P_value	F8	Min	Mean	Max	SD	P_value
FPA	0.15624	0.32455	0.65059	0.13231	3.0199e-11	FPA	-1653.42	-1131.81	-850.42	143.875	7.3891e-11
CFPA1	0.057706	0.12494	0.20889	0.03765	9.5332e-07	CFPA1	-1741.17	-1542.75	-1364.24	105.639	5.1857e-07
CFPA2	0.067287	0.10801	0.18623	0.033423	0.00016813	CFPA2	-1657.24	-1382.22	-1184.77	100.013	9.9186e-11
CFPA3	0.28667	0.99622	2.0141	0.36293	3.0199e-11	CFPA3	-1322.50	-1043.29	-862.753	108.658	3.0199e-11
CFPA4	0.048361	0.11212	0.19141	0.036538	0.0001585	CFPA4	-1643.94	-1488.54	-1334.67	83.792	4.1997e-10
CFPA5	0.062162	0.14842	0.3241	0.062084	2.0283e-07	CFPA5	-1729.71	-1497.70	-1290	100.362	2.4386e-09
CFPA6	0.043699	0.10542	0.19245	0.030208	0.0001325	CFPA6	-1759.15	-1503.80	-1273.80	130.255	1.5964e-07
CFPA7	0.090922	0.16125	0.25181	0.039206	2.8716e-10	CFPA7	-1813.13	-1492.34	-1331.88	106.527	5.4617e-09
CFPA8	0.06351	0.11408	0.21664	0.033287	3.3242e-06	CFPA8	-1789.16	-1626.58	-1421.25	90.0144	0.00117
CFPA9	0.03185	0.07478	0.1562	0.02663	N/A	CFPA9	-1888.13	-1712.25	-1525.25	88.4066	N/A
CFPA10	0.035172	0.099694	0.15984	0.031864	0.0020523	CFPA10	-1702.30	-1475.93	-1291.01	90.456	3.4742e-10
F9	Min	Mean	Max	SD	P_value	F10	Min	Mean	Max	SD	P_value
FPA	1025.9694	2169.5338	2996.8382	511.3697	3.0199e-11	FPA	5.3115	7.5831	9.9519	1.278	3.0199e-11
CFPA1	283.9165	403.1899	545.4251	54.3511	3.1589e-10	CFPA1	4.2955	5.8949	7.3575	0.78624	3.0199e-11
CFPA2	297.7482	411.5311	507.8917	54.5288	1.4643e-10	CFPA2	4.7235	5.782	7.2107	0.57168	3.0199e-11
CFPA3	1980.8766	3366.1027	4991.3019	804.2698	3.0199e-11	CFPA3	11.8103	15.4704	19.3244	1.9464	3.0199e-11
CFPA4	307.0152	391.24	535.5801	55.27	1.3289e-10	CFPA4	4.2618	5.5218	6.9342	0.59866	3.0199e-11
CFPA5	329.1627	393.4048	536.2299	42.2453	4.5043e-11	CFPA5	4.0261	5.686	6.9911	0.73228	3.6897e-11
CFPA6	302.8157	376.3266	448.7993	38.9004	2.6099e-10	CFPA6	3.8597	5.1244	6.3385	0.64606	3.6897e-11
CFPA7	323.1578	424.4181	557.3205	53.0316	3.6897e-11	CFPA7	5.0223	6.298	9.2557	0.92042	3.0199e-11
CFPA8	264.1107	326.2561	401.1862	33.973	5.462e-06	CFPA8	3.3149	4.2157	4.9121	0.43329	2.0338e-09
CFPA9	206.9029	279.2901	346.3255	32.2428	N/A	CFPA9	2.2458	3.0972	4.2158	0.48377	N/A
CFPA10	278.6275	360.4726	463.1863	45.4313	8.4848e-09	CFPA10	3.7075	4.8073	5.9214	0.53391	7.3891e-11

TABLE 6 *(Continued)* Findings of CFPA9 vs. FPA for benchmark functions.

F1	Min	Mean	Max	SD	*p*_value	F2	Min	Mean	Max	SD	*p*_value
F11	Min	Mean	Max	SD	P_value	F12	Min	Mean	Max	SD	P_value
FPA	10.0273	17.1392	31.1986	4.6426	3.0199e-11	FPA	10.0087	160.1734	2890.9879	523.0314	3.0199e-11
CFPA1	1.1884	1.3695	1.7622	0.13387	3.0199e-11	CFPA1	3.2916	5.5136	9.4395	1.4506	8.1527e-11
CFPA2	1.1943	1.5145	2.2726	0.23114	3.0199e-11	CFPA2	3.5414	5.8917	9.3688	1.5095	4.0772e-11
CFPA3	11.5455	25.5432	44.0943	8.0236	3.0199e-11	CFPA3	25.0823	5100.2113	50800.3797	11213.2137	3.0199e-11
CFPA4	1.2056	1.3445	1.5901	0.10144	3.0199e-11	CFPA4	2.3269	4.8953	7.6598	1.3673	1.6947e-09
CFPA5	1.1681	1.4789	2.1694	0.20091	3.0199e-11	CFPA5	2.7669	5.9584	8.8701	1.4442	1.3289e-10
CFPA6	1.0822	1.2914	1.6952	0.13654	3.0199e-11	CFPA6	3.4101	5.1621	9.6344	1.1146	7.3891e-11
CFPA7	1.2083	1.5551	2.2949	0.24763	3.0199e-11	CFPA7	4.2472	7.6579	12.0013	1.9544	3.0199e-11
CFPA8	1.0535	1.0997	1.2496	0.037536	3.0199e-11	CFPA8	1.9255	3.9657	5.5922	1.1247	4.8011e-07
CFPA9	0.8517	1	1.0518	0.042834	N/A	CFPA9	0.82248	2.2613	3.8752	0.83324	N/A
CFPA10	1.0881	1.2361	1.3862	0.088953	3.0199e-11	CFPA10	2.6975	4.6512	6.9048	1.1221	1.5465e-09
F13	Min	Mean	Max	SD	*p*_value						
FPA	769.5354	10.441e04	33.351e04	1.002e05	3.0199e-11						
CFPA1	10.7621	18.0696	25.3133	4.317	4.0772e-11						
CFPA2	9.3378	18.7755	30.6838	5.2009	4.5043e-11						
CFPA3	15.374e03	29.315e04	17.289e05	3.404e05	3.0199e-11						
CFPA4	8.4825	17.1962	24.9967	5.2347	1.4643e-10						
CFPA5	10.5432	20.0204	31.9404	5.7094	4.5043e-11						
CFPA6	8.1749	16.0164	34.4679	5.6702	3.4742e-10						
CFPA7	12.5089	23.8955	39.2147	6.2935	3.0199e-11						
CFPA8	5.2528	12.9477	27.8667	5.1748	3.0811e-08						
CFPA9	1.0607	5.2817	11.99	3.0905	N/A						
CFPA10	5.5711	13.5865	23.4509	4.6388	4.1825e-09						

$$C_{uew,i} = K_{uew,i} \int_{P_{ws,i}}^{P_{wr,i}} \left(p_{w,i} - P_{ws,i}\right) f_w\left(p_{w,i}\right) dp_{w,i} \tag{5}$$

$$C_{oew,i} = K_{oew,i} \int_{0}^{P_{ws,i}} \left(P_{ws,i} - p_{w,i}\right) f_w\left(p_{w,i}\right) dp_{w,i} \tag{6}$$

where $d_{w,i}$ is the coefficient of direct cost of the i^{th} wind generator. $K_{oew,i}$ and $K_{uew,i}$ are the over- and under-estimation cost coefficients pertaining to the i^{th} wind power plant. $p_{ws,i}$ is the scheduled power. $f_w\left(p_{w,i}\right)$ is the probability density function of the i^{th} wind power plant.

2.1.2 Solar power

The probability distribution function used to calculate the PV output power is lognormal distribution, as shown below (Chang, 2010):

$$f(G) = \frac{1}{G\sigma\sqrt{2\pi}} \exp\left[\frac{-(\ln x - \mu)^2}{2\sigma^2}\right], \quad G > 0 \tag{7}$$

The available power $Ps(G)$ of solar irradiation G is determined as follows (Chang, 2010):

$$P_s(G) = \begin{cases} P_{sr}\left(\dfrac{G^2}{G_{std}R_c}\right) 0 < G < R_c \\ P_{sr}\left(\dfrac{G}{G_{std}}\right) R_c \leq G \end{cases} \tag{8}$$

where P_{sr}, G_{std}, G, and R_c are the rated output power of solar PV, solar irradiation in standard environment, forecasted solar irradiation, and certain irradiance point, respectively.The PV's total cost is formulated as follows (Biswas et al., 2017):

$$C_{Ts,is} = C_{ds,is} + C_{ues,is} + C_{oes,is} \tag{9}$$

with

$$C_{ds,i} = d_{s,i} P_{ss,i} \tag{10}$$

$$C_{ues,i} = K_{ues,i} \int_{P_{ss,i}}^{P_{sr,i}} \left(p_{s,i} - P_{ss,i}\right) f_s\left(p_{s,i}\right) dp_{s,i} \tag{11}$$

$$C_{oes,i} = K_{oes,i} \int_{0}^{P_{ss,i}} \left(P_{ss,i} - p_{s,i}\right) f_s\left(p_{s,i}\right) dp_{s,i} \tag{12}$$

where $d_{s,i}$ is the coefficient of direct cost of the i^{th} wind generator. $P_{ss,i}$ is the scheduled power. $K_{oes,i}$ and $K_{ues,i}$ are the over- and under-estimation cost coefficients of the solar power plant. $f_s\left(p_{s,i}\right)$ is the probability density function of the i^{th} solar power plant.

2.2 Optimal power flow model

As mentioned before, the OPF is one of the most significant power system issues. Its major task is recognizing the optimal

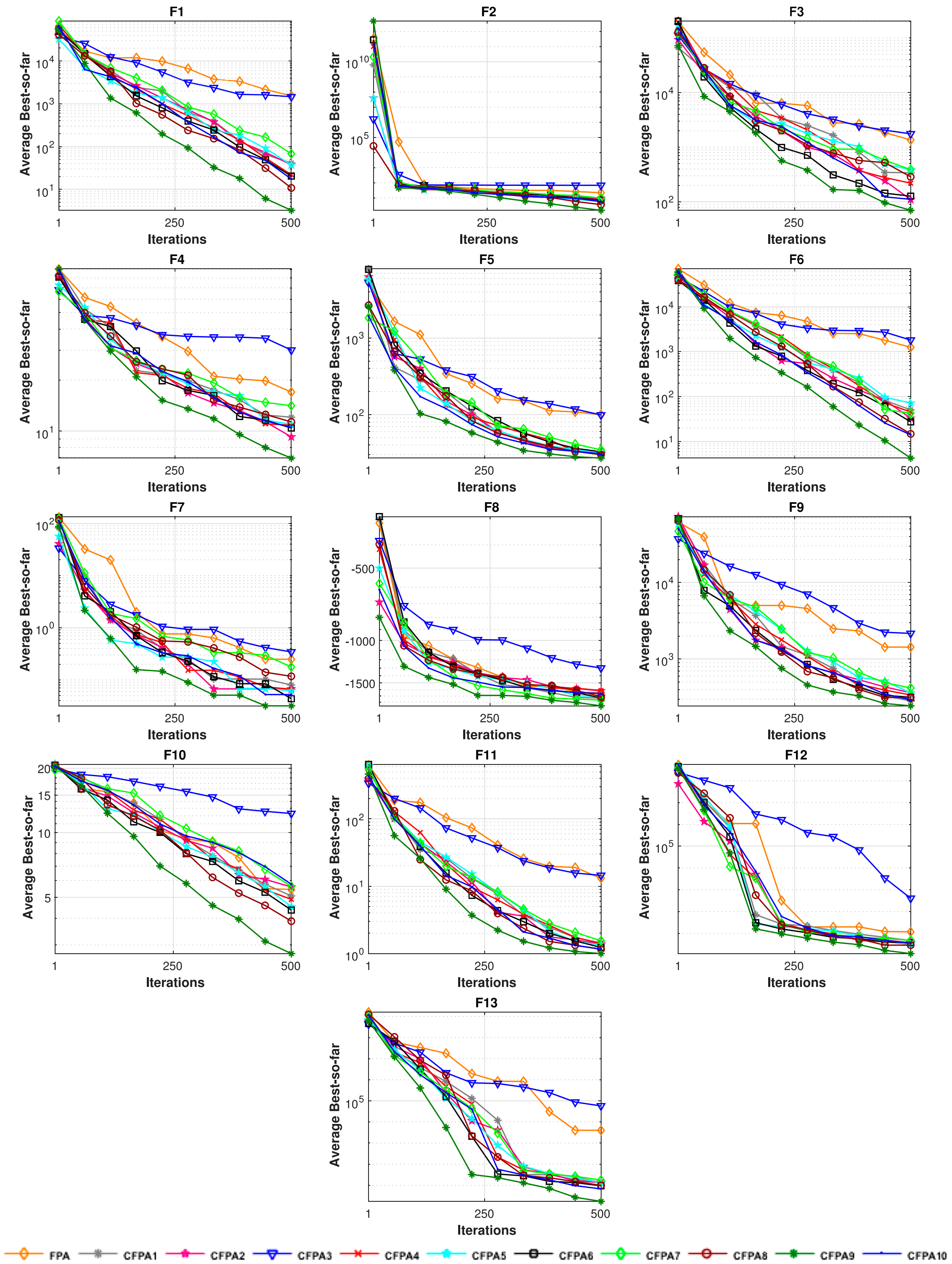

FIGURE 4
Convergence curves for chaotic FPAs on benchmark functions.

TABLE 7 Findings of CFPA9 vs. well-known algorithms for benchmark functions.

Functions		ABC	GOA	DA	FPA	CFPA9
F1	Mean	116.6601	36.7677	2416.3327	1963.2259	**2.9818**
	SD	64.452	23.2903	1613.6725	474.3919	**1.4201**
	*p*_value	3.0199e-11	6.0658e-11	3.0199e-11	3.0199e-11	**N/A**
F2	Mean	46.1637	177.2225	14.8472	29.3898	**1.9905**
	SD	30.146	860.3	4.7841	6.5254	**0.66801**
	*p*_value	4.6159e-10	3.0199e-11	3.0199e-11	3.0199e-11	**N/A**
F3	Mean	69521.8929	2619.8066	16094.2627	1590.9756	**158.4073**
	SD	12499.4266	1502.5193	11378.0237	572.8565	**61.1223**
	*p*_value	3.0199e-11	3.0199e-11	3.0199e-11	3.0199e-11	**N/A**
F4	Mean	62.0671	14.8371	31.1783	23.9382	**8.2198**
	SD	3.8302	4.7927	10.7295	2.7977	**1.5409**
	*p*_value	3.0199e-11	2.6015e-08	3.0199e-11	3.0199e-11	**N/A**
F5	Mean	345.9334	28.433	141.3843	120.9345	**28.093**
	SD	108.852	0.92553	64.046	23.2648	**0.49997**
	*p*_value	3.0199e-11	0.077272	3.0199e-11	3.0199e-11	**N/A**
F6	Mean	112.6667	37.5686	1878.3772	1852.3413	**3.5872**
	SD	75.1871	29.0042	963.0336	491.316	**1.4723**
	*p*_value	3.0199e-11	5.4941e-11	3.0199e-11	3.0199e-11	**N/A**
F7	Mean	1.4799	**0.041089**	0.62517	0.34205	0.065387
	SD	0.52768	**0.014518**	0.39842	0.15655	0.023687
	*p*_value	3.0199e-11	**N/A**	3.0199e-11	3.0199e-11	0.0001325
F8	Mean	**-5.6303e+58**	-1240.4494	-1040.9488	-1095.3226	-1695.7838
	SD	**1.4059e+59**	138.0314	127.9084	108.4415	111.014
	*p*_value	**N/A**	3.0199e-11	3.0199e-11	3.0199e-11	3.0199e-11
F9	Mean	436.0523	443.7524	2665.0095	2274.6595	**280.0637**
	SD	75.9649	159.8135	1238.7848	580.6494	**24.1048**
	*p*_value	3.6897e-11	2.8314e-8	3.0199e-11	3.0199e-11	**N/A**
F10	Mean	7.4231	5.4142	10.8368	7.288	**2.855**
	SD	1.1225	1.2559	1.5819	0.99471	**0.32758**
	*p*_value	3.0199e-11	3.0199e-11	3.0199e-11	3.0199e-11	**N/A**
F11	Mean	2.1745	1.152	19.7806	18.1328	**1.0222**
	SD	0.53328	0.11201	11.4345	4.7354	**0.034169**
	*p*_value	3.0199e-11	7.1186e-09	3.0199e-11	3.0199e-11	**N/A**
F12	Mean	6792882.4494	8.2236	25978.5502	151.4782	**2.5887**
	SD	8644976.7061	17.0986	569127.2029	105867.7541	**2.5436**
	*p*_value	3.0199e-11	1.3289e-10	3.0199e-11	3.0199e-11	**N/A**
F13	Mean	14599925.2831	36.9686	290628.383	103326.9928	**4.853**
	SD	8644976.7061	17.9086	569127.2029	105867.7541	**2.5436**
	*p*_value	3.0199e-11	7.3891e-11	3.0199e-11	3.0199e-11	**N/A**

The bold values indicates the best results.

steady-state operation of power system network components to satisfy the power flow equations and constraints. It is worth noting that the employment of a stochastic technique within power systems has seen important progress over the last few years. The objective functions to be optimized in this work are fuel cost, emission, voltage deviation, and power loss. To this end, the formulation of all variables, objectives, and constraints can be mathematically formulated as follows:

$$\begin{aligned} &Minimize: F(s,c) \\ &Subject\ to: g(s,c)=0 \\ &\qquad h(s,c)\leq 0 \end{aligned} \tag{13}$$

where $F(s,c)$ is the fitness function to be minimized, $g(s,c)$ is the equality constraints, $h(s,c)$ is the inequality constraints, s and c are the vectors of state and control variables.

2.2.1 Variables

The state variables s can be defined as follows (Biswas et al., 2017):

$$s = \left[P_{g1}, V_{L1}, \ldots, V_{LNpq}, Q_{g1}, \ldots, Q_{gNg}, S_{l1}, \ldots, S_{lNl}\right] \tag{14}$$

where P_{g1} is the active power output at the slack bus. V_L is the voltage magnitude at PQ buses. Q_g is the reactive power output of all generator units. S_l is the transmission line loading (line flow). N_{pq}, N_g, and N_l denote the number of load buses, number of generating units, and number of transmission lines, respectively.

The control variables c can be expressed as follows (Biswas et al., 2017):

$$c = \left[P_{g2}, \ldots, P_{gNg}, V_{g1}, \ldots, V_{gNg}, Q_{c1}, \ldots, Q_{cNc}, T_1, \ldots, T_{NT}\right] \tag{15}$$

where P_g is the active power generation at the PV buses, except at the slack bus. V_g is the generation bus voltage magnitude at

PV buses. T is the transformer tap settings. Q_c is the shunt *VAR* compensation. N_g, N_c, and N_T are the number of generators, number of regulating transformers, and number of *VAR* (shunt) compensators, respectively.

2.2.2 Objective functions

In this division, five fitness functions are considered as objectives:

2.2.2.1 Fuel cost only

The conventional generator total fuel cost of the network is modeled as a quadratic function, and its formulation can be expressed as follows (Biswas et al., 2017):

$$F_1 = F_c(s,c) = min\left\{\sum_{i=1}^{Ng} a_i + b_i P_{gi} + c_i P_{gi}^2 + |d_i * sin\left(e_i * \left(P_{gi}^{min} - P_{gi}\right)\right)|\right. \quad (16)$$

where a_i, b_i, c_i, d_i, and e_i are the conventional generator cost coefficients.

2.2.2.2 Emission

The emission function is formulated using an exponential function and the previous quadratic function as shown below (Biswas et al., 2017):

$$F_2 = E(s,c) = min\left\{\sum_{i=1}^{Ng} 10^{-2}\left(\alpha_i + \beta_i P_{gi} + \gamma_i P_{gi}^2\right) + \xi_i \exp\left(\lambda_i P_{gi}\right)\right. \quad (17)$$

where α_i, β_i, γ_i, ξ_i, and λ_i are the emission coefficients of the power plant.

2.2.2.3 Fuel cost with renewable energy cost

The network total cost including the wind-solar-thermal powers is expressed as follows (Biswas et al., 2017):

$$F_3 = min\left\{F_1 + C_{Tw,iw} + C_{Ts,is}\right. \quad (18)$$

The voltage deviation and power loss are also important in the power system. These two functions are calculated as shown below.

2.2.2.4 Voltage deviation

The load bus voltages are picked from 1.0 per unit in order to grab the problem of an unattractive voltage profile. The voltage deviation can be defined as follows (Elattar and ElSayed, 2019):

$$F_4 = VD(s,c) = min\left\{\ \sum_{i=1}^{Npq}|V_{Li} - 1.0|\right. \quad (19)$$

2.2.2.5 Power loss

The transmission system power losses are necessary due to the inherent resistance of lines. Its mathematical modeling is formulated by the following expression (Elattar and ElSayed, 2019):

$$F_5 = P_{loss}(s,c) = min\left\{\ \sum_{l=1}^{N_l} G_{l(i,j)}\left(V_i^2 + V_j^2 - 2V_iV_j cos\left(\delta_{ij}\right)\right)\right. \quad (20)$$

where $G_{l(i,j)}$ represents the conductance of line l. $\delta_{ij} = \delta_i - \delta_j$ represents the voltage angle difference between bus i and bus j.

2.2.3 Constraints

The equality and inequality constraints play an important role in optimal power flow studies; they stand for the limitations of physical equipment. These constraints have been modeled as shown below.

2.2.3.1 Equality constraints

The power flow equations are assumed as equality constraints that are represented by the following (Elattar and ElSayed, 2019):

$$\begin{cases} P_{gi} - P_{di} - |V_i|\sum_{j=1}^{Nb}|V_j|\left[G_{ij}cos\left(\theta_{ij}\right) + B_{ij}sin\left(\theta_{ij}\right)\right] = 0 \\ Q_{gi} - Q_{di} - |V_i|\sum_{j=1}^{Nb}|V_j|\left[G_{ij}sin\left(\theta_{ij}\right) - B_{ij}cos\left(\theta_{ij}\right)\right] = 0 \end{cases} \quad (21)$$

where Nb is the number of buses. Q_{gi} and P_{gi} are generated reactive and active power, respectively. Q_{di} and P_{di} are reactive and active power demand, respectively. G_{ij} and B_{ij} represent the admittance matrix components $Y_{ij} = G_{ij} + jB_{ij}$ named conductance and susceptance.

2.2.3.2 Inequality constraints

The inequality constraints are given as shown below (Elattar and ElSayed, 2019):

– Generator constraints:

$$V_{gi}^{min} \le V_{gi} \le V_{gi}^{max} \qquad i = 1, \ldots, Ng \quad (22)$$

$$P_{gi}^{min} \le P_{gi} \le P_{gi}^{max} \qquad i = 1, \ldots, Ng \quad (23)$$

$$P_{ws,i}^{min} \le P_{ws,i} \le P_{ws,i}^{max} \qquad i = 1, \ldots, Nwg \quad (24)$$

$$P_{ss,i}^{min} \le P_{ss,i} \le P_{ss,i}^{max} \qquad i = 1, \ldots, Nsg \quad (25)$$

$$Q_{gi}^{min} \le Q_{gi} \le Q_{gi}^{max} \qquad i = 1, \ldots, Ng \quad (26)$$

$$Q_{ws,i}^{min} \le Q_{ws,i} \le Q_{ws,i}^{max} \qquad i = 1, \ldots, Nwg \quad (27)$$

$$Q_{ss,i}^{min} \le Q_{ss,i} \le Q_{ss,i}^{max} \qquad i = 1, \ldots, Nsg \quad (28)$$

where V_i^{min} and V_i^{max} indicate the minimum and maximum limits of the bus voltage. P_{gi}^{min} and P_{gi}^{max} represent the lower and upper bounds of the active power generator. Q_{gi}^{min} and Q_{gi}^{max} are the minimum and maximum reactive power limits of the generator. $P_{ws,i}^{min}$, $P_{ws,i}^{max}$, $P_{ss,i}^{min}$, $P_{ss,i}^{max}$, $Q_{ws,i}^{min}$, $Q_{ws,i}^{max}$, $Q_{ss,i}^{min}$, and $Q_{ss,i}^{max}$ are the bounds of energy resources. Ng, Nwg, and Nsg are the number of generations, wind and solar, respectively.

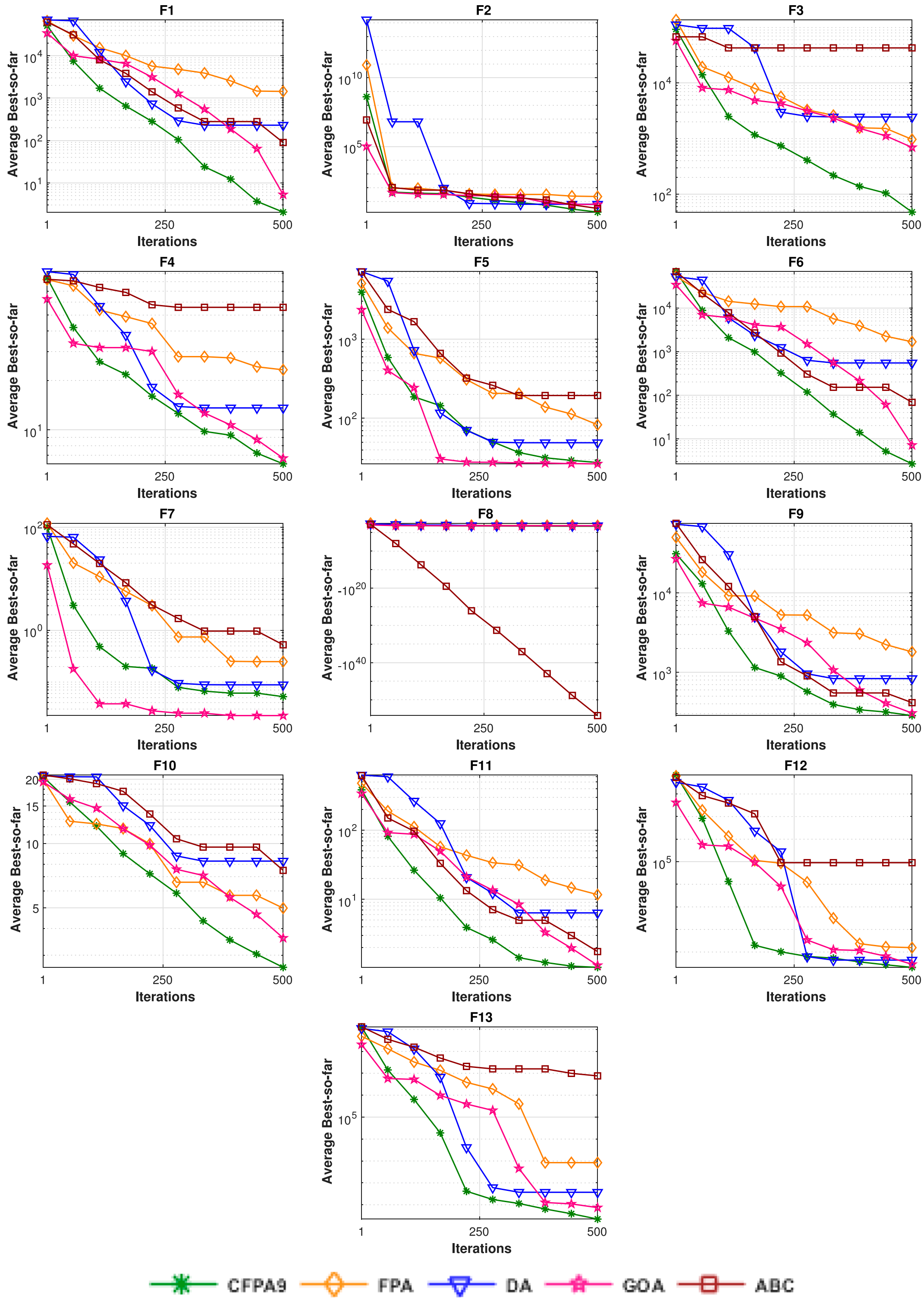

FIGURE 5
Convergence curves of CFPA9 vs. well-known approaches for benchmark functions.

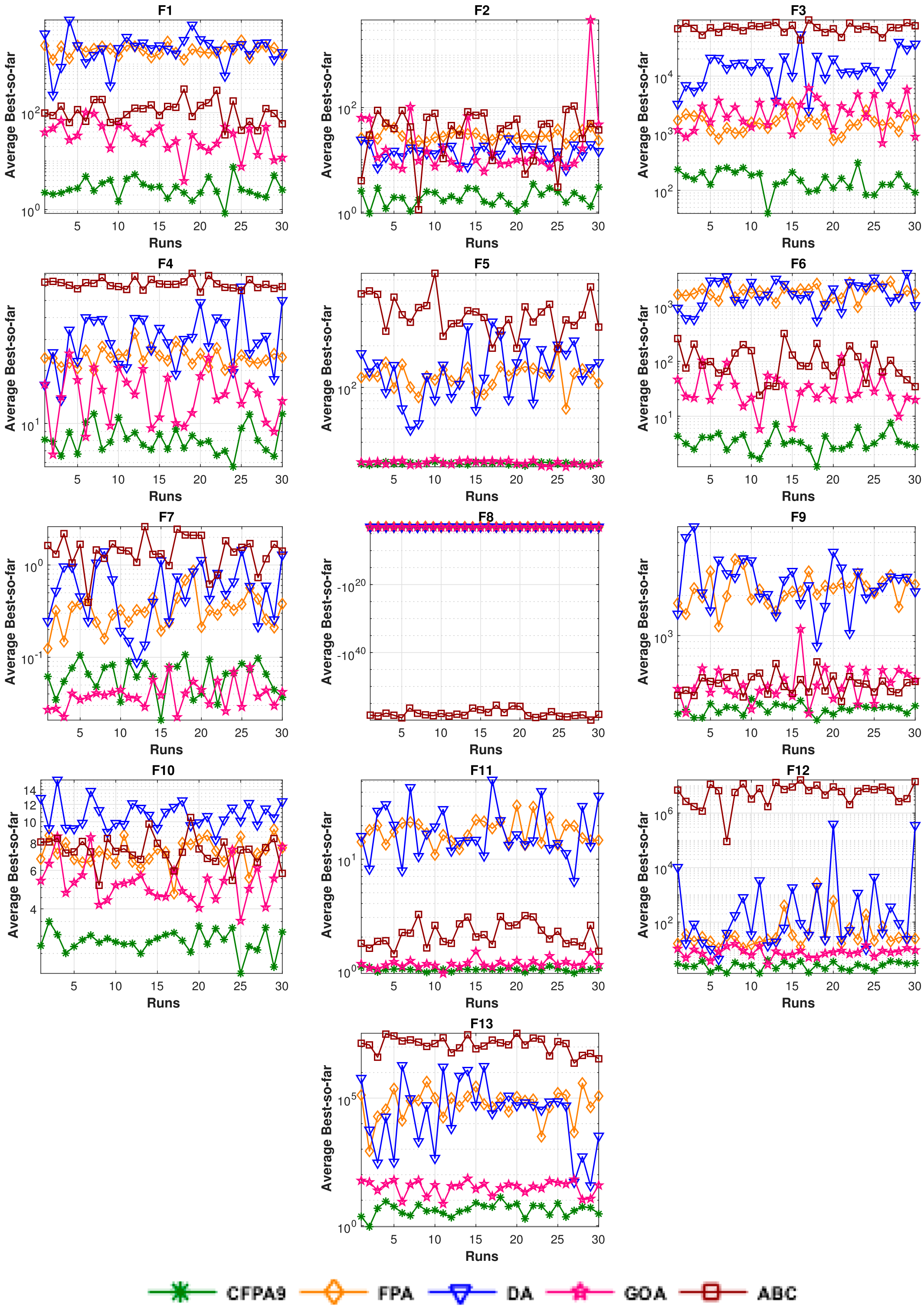

FIGURE 6
Runs of best CFPA9 versus well-known algorithms.

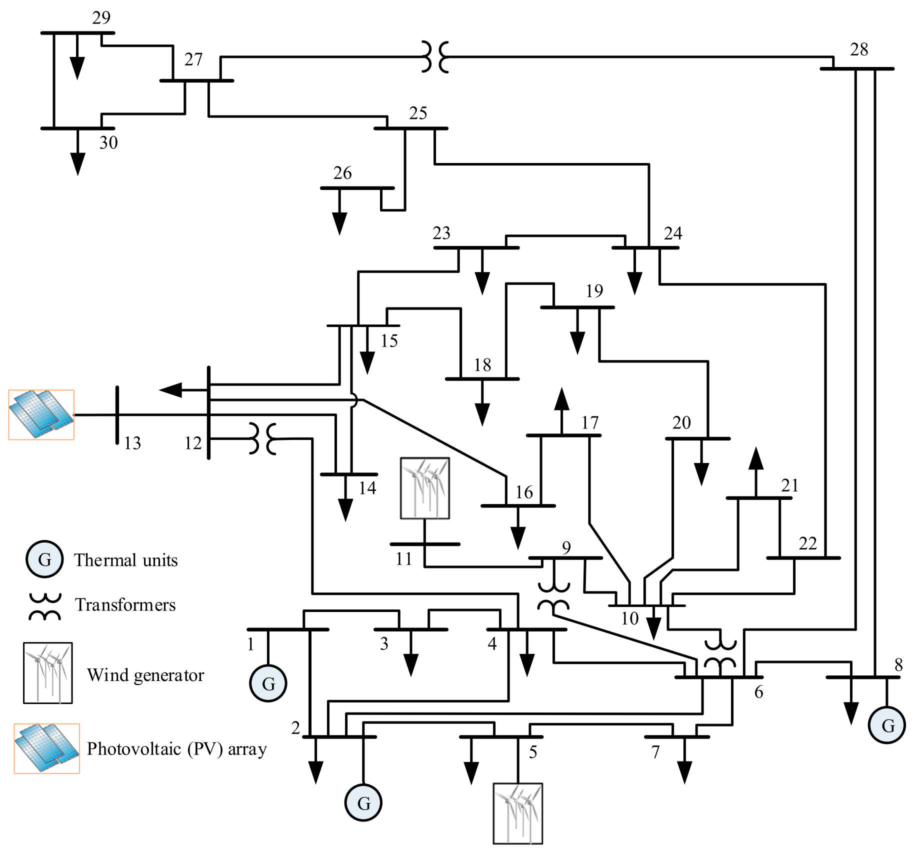

FIGURE 7
Single-line diagram of the IEEE 30-bus test system with wind and solar power.

– Transformer constraints:

$$T_i^{min} \le T_i \le T_i^{max} \qquad i = 1, \ldots, N_T \tag{29}$$

where N_T is the number of tap changer transformers. T_i^{min} and T_i^{max} represent the minimum and maximum limits of the transformer, respectively.

– Shunt VAR compensator constraints:

$$Q_{ci}^{min} \le Q_{ci} \le Q_{ci}^{max} \qquad i = 1, \ldots, Nc \tag{30}$$

where Nc is the number of capacitor components. $Q_{c,i}^{min}$ and $Q_{c,i}^{max}$ are the minimum and maximum limits of the shunt compensators.

– Security constraints:

$$V_{Li}^{min} \le V_{Li} \le V_{Li}^{max} \qquad i = 1, \ldots, Npq \tag{31}$$

$$S_{li} \le S_{li}^{max} \qquad i = 1, \ldots, Nl \tag{32}$$

where Nl is the number of transmission lines. S_{li} and S_{li}^{max} indicate the maximum limit of the transmission line.

3 Optimization methodology

3.1 Flower pollination algorithm

Flower pollination algorithm (FPA) is a stochastic approach in the field of swarm intelligence algorithms. It was proposed for solving nonlinear single-objective optimization problems by Xin-She Yang in 2012 (Yang, 2012). As its name signifies, FPA is inspired by the flower pollination process. Besides, the transfer of pollen generally leads to flower pollination, and this transfer is often associated with some pollinators such as butterflies, bats, birds, etc. As a matter of fact, certain insects and flowers have developed a very specialized flower–pollinator partnership (Yang, 2014). Generally speaking, the pollination process can be categorized into two sorts of pollination: cross-pollination and self-pollination. The self-pollination or abiotic pollination transfers the pollen itself without requiring any pollinators; thus, this process is used for local pollination. Meanwhile, cross or biotic pollination requires pollinators to transfer the pollen from one plant to another, and these pollinators carrying pollen move in a way that obeys the distribution of the Lévy

TABLE 8 Findings for case 1 and case 2 (IEEE 30-bus).

Case 1 Control variables	Min	Max	FPA	CFPA9	Case 2 Control variables	Min	Max	CFPA9
P_{g2}	20	80	48.1132	48.5164	P_{g2}	20	80	40.9239
P_{g5}	15	50	22.8765	21.3983	P_{ws1}	0	75	37.5287
P_{g8}	10	35	20.2906	21.0749	P_{g8}	10	35	10.0000
P_{g11}	10	30	10.0014	12.0981	P_{ws2}	0	60	17.6498
P_{g13}	12	40	12.4070	12.0000	P_{ss}	0	50	49.9846
V_{g1}	0.95	1.1	1.0999	1.0999	V_{g1}	0.95	1.1	1.10000
V_{g2}	0.95	1.1	1.0897	1.0883	V_{g2}	0.95	1.1	1.0869
V_{g5}	0.95	1.1	1.0568	1.0616	V_{g5}	0.95	1.1	1.0620
V_{g8}	0.95	1.1	1.0652	1.0717	V_{g8}	0.95	1.1	1.0645
V_{g11}	0.95	1.1	1.0799	1.0974	V_{g11}	0.95	1.1	1.0928
V_{g13}	0.95	1.1	1.0876	1.0979	V_{g13}	0.95	1.1	1.10000
Q_{c10}	0	5	1.6304	4.4487	Q_{c10}	0	5	5.0000
Q_{c12}	0	5	3.2084	4.7963	Q_{c12}	0	5	2.7045
Q_{c15}	0	5	3.7831	4.1751	Q_{c15}	0	5	3.5921
Q_{c17}	0	5	5.0000	4.9658	Q_{c17}	0	5	3.2589
Q_{c20}	0	5	3.9598	4.8145	Q_{c20}	0	5	0.0000
Q_{c21}	0	5	3.0930	3.7935	Q_{c21}	0	5	1.1542
Q_{c23}	0	5	0.9155	3.9068	Q_{c23}	0	5	2.7377
Q_{c24}	0	5	4.8312	5.0000	Q_{c24}	0	5	2.1904
Q_{c29}	0	5	2.6265	1.3365	Q_{c29}	0	5	3.2935
T_{11}	0.9	1.1	1.0470	1.0392	T_{11}	0.9	1.1	1.0306
T_{12}	0.9	1.1	0.9059	0.9088	T_{12}	0.9	1.1	0.9000
T_{15}	0.9	1.1	1.0367	0.9835	T_{15}	0.9	1.1	0.9559
T_{36}	0.9	1.1	0.9542	0.9594	T_{36}	0.9	1.1	0.9661
Fuel cost ($/h)	-	-	799.6144	**798.9867**	Total cost ($/h)	-	-	**696.9185**
Wind cost ($/h)	-	-	-	-	Wind cost ($/h)	-	-	**173.4157**
PV cost ($/h)	-	-	-	-	PV cost ($/h)	-	-	**56.0963**
E (ton/h)	-	-	0.3701	**0.3656**	E (ton/h)	-	-	0.1557
VD (p.u.)	-	-	0.9057	**0.4969**	VD (p.u.)	-	-	0.6845
$P_{loss}(MW)$	-	-	8.7543	**8.5794**	$P_{loss}(MW)$	-	-	5.9584
P_{g1}	50	200	178.4656	176.8915	P_{g1}	50	140	133.2713
CPU time (s)	-	-	61.8980	68.0380	CPU time (s)	-	-	153.625

The bold values indicates the best results.

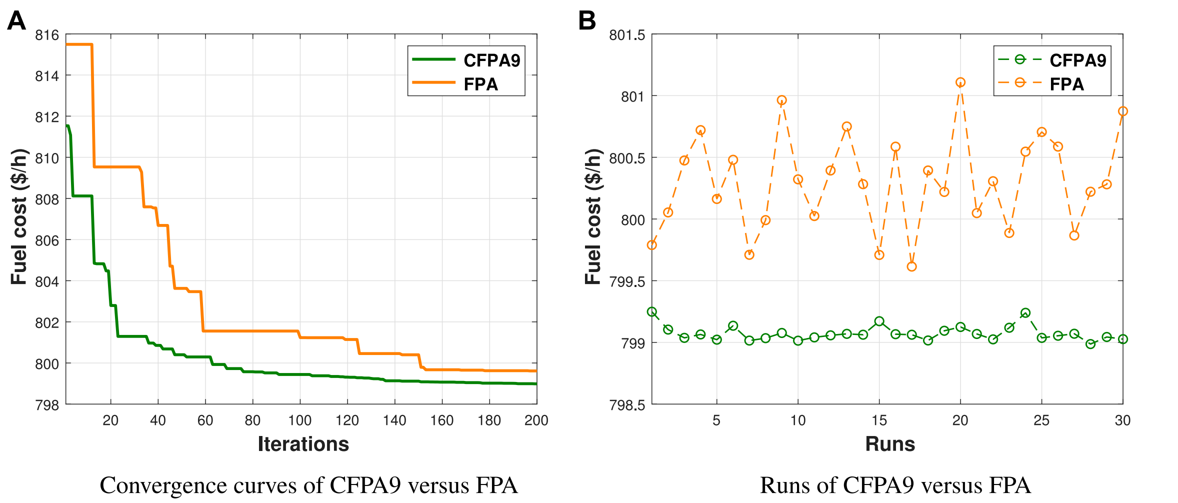

FIGURE 8
Fuel cost convergence and run for FPA vs. CFPA9 for case 1. **(A)** Convergence curves of CFPA9 versus FPA and **(B)** runs of CFPA9 versus FPA.

TABLE 9 Comparison analysis of 30-bus and 57-bus test system case 1 and case 3.

Approaches	30-bus	57-bus
CFPA9	**798.9867**	**41 631.2601**
FPA	799.6144	41 666.432
BSA Chaib et al. (2016)	799.0760	-
GEM Bouchekara et al. (2016a)	799.0463	-
ALO Trivedi et al. (2016)	799.155	-
MSA Mohamed et al. (2017)	800.5099	41 673.721
NISSO Nguyen, (2019)	798.9936	41 665.54
ICBO Bouchekara et al. (2016b)	799.0353	-
MSA–GSA Shilaja and Arunprasath, (2019)	799.01	41 658.58
ECHT-DE Biswas et al. (2018a)	800.4131	41 667.82
IMFO Taher et al. (2019a)	800.3848	41 667.1497
DSA Abaci and Yamacli, (2016)	800.3887	41 686.82
ISA Bentouati et al. (2017)	799.2776	41 676.9466
IEM Bouchekara et al. (2016c)	799.1821	41 810.261
TSA El-Fergany and Hasanien, (2018)	-	41 685.07
LAPO Taher et al. (2019b)	800.59	-
AGOA Alhejji et al. (2020)	800.0212	-
AMTPG-Jaya Warid, (2020)	800.1946	-
SOS Duman, (2017)	801.5733	-

The bold values indicates the best results.

flights (Pavlyukevich, 2007). This type of pollination can be recognized as global pollination. Moreover, the global and local pollination are controlled using a random parameter p called switch probability in which its value is in the range $[0,-,1]$. The mathematical representation of these two processes is given below:

- The global pollination is governed by the following (Yang, 2012):

$$x_i^{t+1} = x_i^t + \gamma L(\lambda)\left(g_{best} - x_i^t\right) \tag{33}$$

where x_i^t denotes the solution vector i at iteration t, γ is the scaling factor, g_{best} indicates the best solution obtained at the actual iteration, and $L(\gamma)$ represents the step size parameter. The Lévy flight distribution is formulated as follows (Yang, 2012):

$$L\sim\frac{1}{s^{1+\lambda}}\frac{\lambda\Gamma(\lambda)\sin(\pi\lambda/2)}{\pi}, \qquad (0 < s_0 \ll s) \tag{34}$$

where $\Gamma(\lambda)$ is the gamma function distribution (Yang, 2014) that is valid for $0 \ll s$. The s_0 expression with the Gaussian distributions U and V are as shown below:

$$s = \frac{U}{|V|^{1/\lambda}}, \qquad V\sim N(0,1), \qquad U\sim N\left(0,\sigma^2\right) \tag{35}$$

where $N(0,\sigma^2)$ and $N(0,1)$ signify a zero mean for both U and V and a variance of σ^2 for U and 1 for V. The variance can be calculated by the following (Yang, 2014):

$$\sigma^2 = \left[\frac{\sin(\pi\lambda/2)}{2^{(\lambda-1)/2}}\frac{\Gamma(1+\lambda)}{\lambda\Gamma((1+\lambda)/2)}\right]^{1/\lambda} \tag{36}$$

- The local pollination process is represented by the following (Yang, 2012):

$$x_i^{t+1} = x_i^t + \epsilon\left(x_j^t - x_k^t\right) \tag{37}$$

where x_j^t and x_k^t indicate the pollen produced from the same plant and dissimilar flowers. ϵ represents a random value which is bounded by 0 and 1.

Selecting FPA is due to its tendency to search both global and local search space, its easiness of implementation, and its small number of parameters. This method is efficient in dealing with the problems which have lower dimensions; in contrast, it faces some difficulties in handling the higher-dimensional constrained optimization issues. Therefore, to tackle these complications, a chaotic method is suggested in the next section.

3.2 Chaos theory

Generally, chaos theory is a deterministic technique observed in the dynamical and nonlinear systems, which are bounded, non-convergent, and non-periodic. The chaos utilizes chaotic variables instead of random variables (Arora and Singh, 2017), which means a small change in its initial conditions may change its future behavior. Besides, owing to the ergodicity properties of chaos and its non-repetition, its use can be more advantageous. Furthermore, in recent years, chaotic sequences have been widely employed in several optimization subject areas due to the fact that they possess the ability to enhance global convergence and avoid the local minimum (Letellier, 2019). For that reason, ten well-known chaos sequences are chosen in this research work, as depicted in **Figure 3** (Sayed et al., 2017). Their names, mathematical expressions, and ranges are listed in **Table 4**.

3.3 Constraint handling superiority of feasible solutions

SF is a constrained handling strategy based on the dominant relationship. This concept is used by Deb (Deb, 2000) in order to handle the superiority of feasible solutions on infeasible ones. The feasible candidate can always dominate the infeasible one, while the candidate with the smaller violation degree always dominates the one with the higher violation value. The SF technique uses a tournament selection operator, where two solutions are compared at a time. Solution X_i is considered superior to X_j if

- An infeasible solution X_j is dominated by a feasible one X_i
- if both X_i, X_j are feasible, but X_j is worse than X_i
- if both X_i, X_j are infeasible, and X_j has the greatest constraint violation.

Referring to Eq. 13, the equality constraints are converted to inequality constraints, and thus, total constraint is introduced as follows (Deb, 2000):

$$H_i(X) = \begin{cases} \max(h_i(X), 0) \\ \max(|g_i(X)| - \delta, 0) \end{cases} \tag{38}$$

where δ is a tolerance parameter for the equality constraints, and $H_i(X)$ is the inequality constraint.

The overall expression of the constraint violation for an infeasible solution can be summarized as follows (Deb, 2000):

$$V(X) = \frac{\sum_{i=1}^{g} w_i (H_i(X))}{\sum_{i=1}^{g} w_i}, \qquad w_i = \frac{1}{H_{max,i}} \tag{39}$$

where w_i is a weight parameter, and $H_{\max,i}$ is the maximum value for violation of constraint.

3.4 Chaotic flower pollination algorithm based SF

All the previous studies prove that FPA gets trapped in local optima and converges slowly toward the minimal solutions. Therefore, in order to make FPA an efficient algorithm, it should properly balance between the diversification and intensification to approximate the global optima. As was pointed out earlier, p is the main parameter of FPA, which balances these two components of the pollination, and it influences the algorithm convergence speed. In this present study, chaotic maps are suggested to deal with these shortcomings and enrich the search behavior due to the fact that chaos sequences can help swarm algorithms to get rid of the local optimum. The proposed chaotic flower pollination algorithm is a hybrid method that tunes the parameter of FPA by replacing random values with chaotic variables. In addition, the chaos is applied to manipulate the local pollination and the switch probability p. This parameter is considered as a single parameter in standard FPA, but in this study, p is proportionally decreased by increasing the iteration numbers; it is modified as follows:

$$p = p_{max} + t\frac{p_{max} - p_{min}}{T} \tag{40}$$

where T characterizes the maximum value of iterations, and t signifies the actual iteration value. $p_{min} = 0.6$ and $p_{max} = 0.8$ indicate the minimum and maximum value of p, respectively.

The proposed approach based on FPA, chaos, and SF is described in Algorithm 1. The rand values in the basic FPA are substituted in CFPA-SF by the chaotic sequence values to supply chaos behaviors as shown in steps 9 and 13 in the pseudo-code, where $C(t)$ is the chaotic sequence value of the t^{th} iteration.

1: Initialize the chaotic FPA parameters (Iterations(MaxIter), population size(nPop), bounds(Ub, Lb), dimension(d), switch probability(p_{min},p_{max}), chaotic maps(C))
2: Generate the random initial population of flowers x respect to Ub and Lb: $x = Lb + rand*(Ub - Lb)$
3: Compute the optimal value, constraint violations in the initial population using Equations (38) and (39)
4: Generate random numbers using chaotic maps(C)
5: Determine the switch probability Equation (40), $p \in [p_{min}, p_{max}]$: $p = p_{max} + t\frac{p_{max}-p_{min}}{MaxIter}$
6: **while** $t < MaxIter$ (stopping criteria) **do**
7: Update parameter values for SF constraint handling technique
8: **for** $i = 1 : nPop$ **do**
9: **if** $C(t) < p$ **then**
10: Draw the step size parameter L which obeys lévy distribution
11: proceed global pollination through Equation (33), $x_i^{t+1} = x_i^t + \gamma\, L(\lambda)\left(g_{best} - x_i^t\right)$
12: **else**
13: Draw ϵ from chaotic maps through $\epsilon = C(t)$
14: proceed local pollination through Equation (37), $x_i^{t+1} = x_i^t + C(t)\left(x_j^t - x_k^t\right)$
15: **end if**
16: Compute the new optimal fitness value, total constraint violations using Equations (38) and (39)
17: If new solution is better, update it in the population
18: **end for**
19: Update the current global best solution
20: **end while**
21: Extract the optimal solution reached

Algorithm 1. Chaos Flower Pollination Algorithm based SF (CFPA-SF).

4 Experimental results

4.1 Simulation results of benchmark functions

In this subsection, all the outcomes are averaged over 30 independent runs, for 13 test suites that have 30 dimensions. The population size considered for all functions is $nPop = 30$, the maximum iteration number is fixed at $T = 500$, and the switch probability value is set at $p = 0.8$ for the traditional FPA. All the

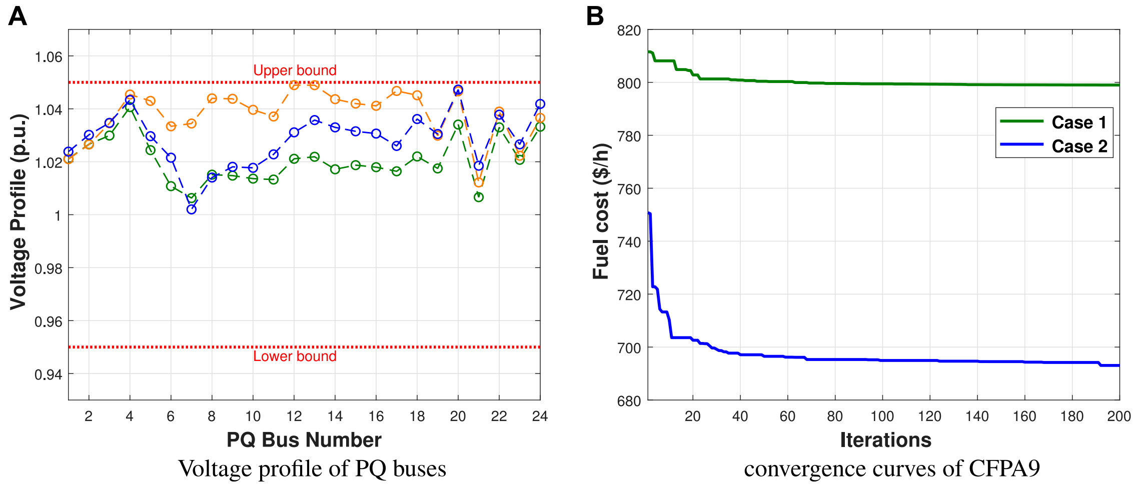

FIGURE 9
Voltage profile and convergence curves of CFPA9 for cases 1 and 2. **(A)** Voltage profile of PQ buses and **(B)** convergence curves of CFPA9.

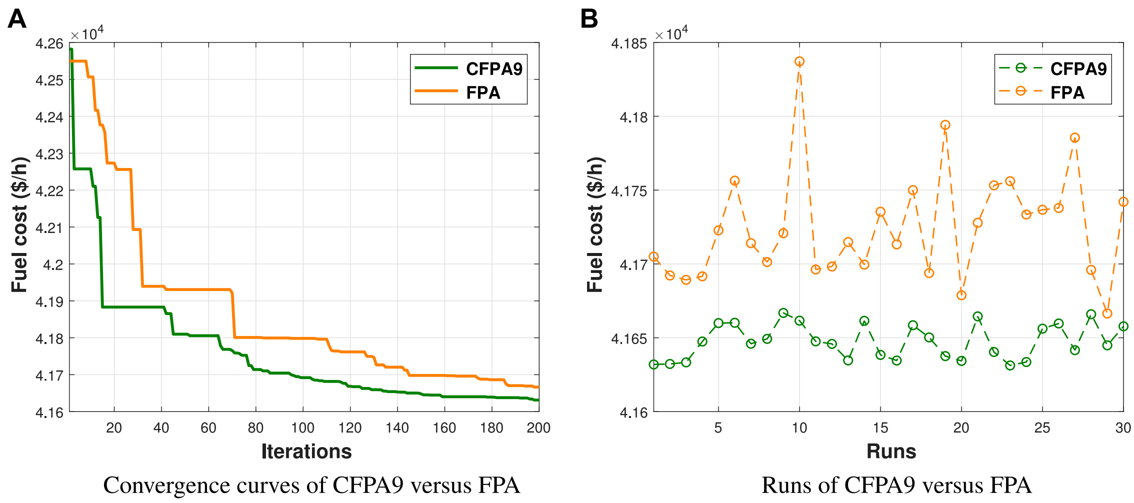

FIGURE 10
Fuel cost convergence and runs for FPA vs. CFPA9 for case 3. **(A)** Convergence curves of CFPA9 versus FPA and **(B)** runs of CFPA9 versus FPA.

approaches are executed on a personal computer core i5 with a 4 GB-RAM Processor @1.8*GHz* using MATLAB R2016b.

The 13 test functions are utilized in order to prove the performance of the suggested approach CFPA. Their details are tabulated in Table 5, where D and Bound represent the dimension (number of variables) and limits of variables, respectively. Additionally, these test suites are classified into four types: multimodal, unimodal, separable, and non-separable. Thus, the multimodal functions are more suitable for assessing the potential performances of algorithms' exploration, although the exploitation capability can generally be checked using the unimodal functions. Therefore, to demonstrate which of the ten CFPAs is significantly improved compared to the standard FPA, five different testing parameters were investigated including the *Min*, *Max*, and *Mean* fitness values, *p_value* of Wilcoxon's rank sum test, and standard deviation (SD) (Wilcoxon, 1945), (Derrac et al., 2011). The *p_value* less than 5% implies the significant improvement of the algorithm and determines which chaotic sequence is the best. As shown in Table 6, the optimal findings are shown in bold text, while the N/A indicates "not applicable," meaning that the best chaotic map could not statistically be compared with itself.The experimental results provide that all CFPA algorithms are much superior to the classical FPA except CFPA3 (Gausse/mouse map). Moreover,

TABLE 10 Findings for case 3 and case 4 (IEEE 57-bus).

Case 3					Case 4			
Control variables	**Min**	**Max**	**FPA**	**CFPA9**	**Control variables**	**Min**	**Max**	**CFPA9**
P_{g2}	30	100	88.9994	85.8167	P_{ws1}	0	150	149.9996
P_{g3}	40	140	48.4887	46.2558	P_{g3}	40	140	42.6342
P_{g6}	30	100	69.5516	71.2833	P_{ws2}	0	150	149.8641
P_{g8}	100	550	482.0487	466.273	P_{g8}	100	550	287.2991
P_{g9}	30	100	76.941	83.1664	P_{ss}	0	120	119.9556
P_{g12}	100	410	352.9002	366.6004	P_{g12}	100	410	371.0457
V_{g1}	0.95	1.1	1.0995	1.0999	V_{g1}	0.95	1.1	1.0694
V_{g2}	0.95	1.1	1.1000	1.1000	V_{g2}	0.95	1.1	1.0787
V_{g3}	0.95	1.1	1.0960	1.0941	V_{g3}	0.95	1.1	1.0608
V_{g5}	0.95	1.1	1.0861	1.0981	V_{g5}	0.95	1.1	1.0677
V_{g8}	0.95	1.1	1.0989	1.0998	V_{g8}	0.95	1.1	1.0535
V_{g9}	0.95	1.1	1.0968	1.0963	V_{g9}	0.95	1.1	1.0366
V_{g12}	0.95	1.1	1.0847	1.0837	V_{g12}	0.95	1.1	1.0420
Q_{c18}	0	20	9.1497	9.7812	Q_{c18}	0	20	7.1993
Q_{c25}	0	20	16.0636	8.0581	Q_{c25}	0	20	417.7231
Q_{c53}	0	20	15.4616	7.4129	Q_{c53}	0	20	11.3146
T_{19}	0.9	1.1	0.9902	0.9282	T_{19}	0.9	1.1	1.0608
T_{20}	0.9	1.1	0.9877	1.0846	T_{20}	0.9	1.1	1.0990
T_{31}	0.9	1.1	1.0061	1.0309	T_{31}	0.9	1.1	1.0101
T_{35}	0.9	1.1	1.0050	0.9000	T_{35}	0.9	1.1	0.9573
T_{36}	0.9	1.1	0.9815	0.9509	T_{36}	0.9	1.1	0.9970
T_{37}	0.9	1.1	0.9880	0.9952	T_{37}	0.9	1.1	1.1000
T_{41}	0.9	1.1	0.9707	0.9489	T_{41}	0.9	1.1	1.0587
T_{46}	0.9	1.1	1.9377	0.9162	T_{46}	0.9	1.1	0.9149
T_{54}	0.9	1.1	1.0698	0.9697	T_{54}	0.9	1.1	0.9737
T_{58}	0.9	1.1	1.0031	0.9813	T_{58}	0.9	1.1	0.9831
T_{59}	0.9	1.1	1.0094	0.9741	T_{59}	0.9	1.1	0.9501
T_{65}	0.9	1.1	0.9469	0.9923	T_{65}	0.9	1.1	0.9385
T_{66}	0.9	1.1	0.9397	0.9631	T_{66}	0.9	1.1	0.9000
T_{71}	0.9	1.1	0.9958	1.0892	T_{71}	0.9	1.1	1.0862
T_{73}	0.9	1.1	0.9938	1.0699	T_{73}	0.9	1.1	1.0514
T_{76}	0.9	1.1	0.9700	1.0116	T_{76}	0.9	1.1	1.0976
T_{80}	0.9	1.1	0.9967	0.952	T_{80}	0.9	1.1	0.9836
Fuel cost ($/h)	-	-	41 666.432	**41 631.2601**	Total cost ($/h)	-	-	**27848.7724**
Wind cost ($/h)	-	-	-	-	Wind cost ($/h)	-	-	**1411.738**
PV cost ($/h)	-	-	-	-	PV cost ($/h)	-	-	**1230.2283**
E (ton/h)	-	-	1.4192	**1.3858**	E (ton/h)	-	-	0.8075
VD (p.u.)	-	-	1.7126	**1.6877**	VD (p.u.)	-	-	1.7277
$P_{loss}(MW)$	-	-	15.2661	**13.8706**	$P_{loss}(MW)$	-	-	13.2593
P_{g1}	0	576	147.1365	145.2737	P_{g1}	0	576	143.2610
CPU time (s)	-	-	72.433	67.251	CPU time (s)	-	-	168.332

The bold values indicates the best results.

it can be observed that the outcomes of CFPA9 (Sinusoidal map) occupied the first rank on all types of test functions compared to the original FPA and its other chaotic variants. Besides, as it is apparent, most of the obtained Wilcoxon rank-sum test (*p*-values) are less than the assumed significant level of 5% compared to other approaches, which means that the combination of the sinusoidal map with FPA enhances the performance of the FPA approach. The fastest convergence rates toward the global optimum shown in Figure 4 guarantee its improvement. Also, this figure indicates that the FPA and CFPA3 algorithms supply the worst solution. Furthermore, to better validate the efficiency of our proposed hybrid method, the performance of the Sinusoidal map based on the statistical mean is compared with the fitness values of three state-of-the-art algorithms, such as DA, GOA, and ABC, as illustrated in Table 7. It bears mentioning that the optimal statistical results of each testing parameter are the lowest values. The bold values designate the optimum solutions. These numerical findings obviously show that the CFPA9 ranks first for the various types of the benchmark suite by supplying 11 significant solutions out of 13 test functions. Meanwhile, ABC and GOA each rank first for one function, F8 and F7, respectively. Despite the fact that CFPA9 fails to reach the optimum results for some functions, it holds second place. By contrast, the DA approach achieves the worst outcomes in most cases. Consequently, as it can be seen from the evolution curve's fitness value shown in Figure 5, CFPA9 converges faster than

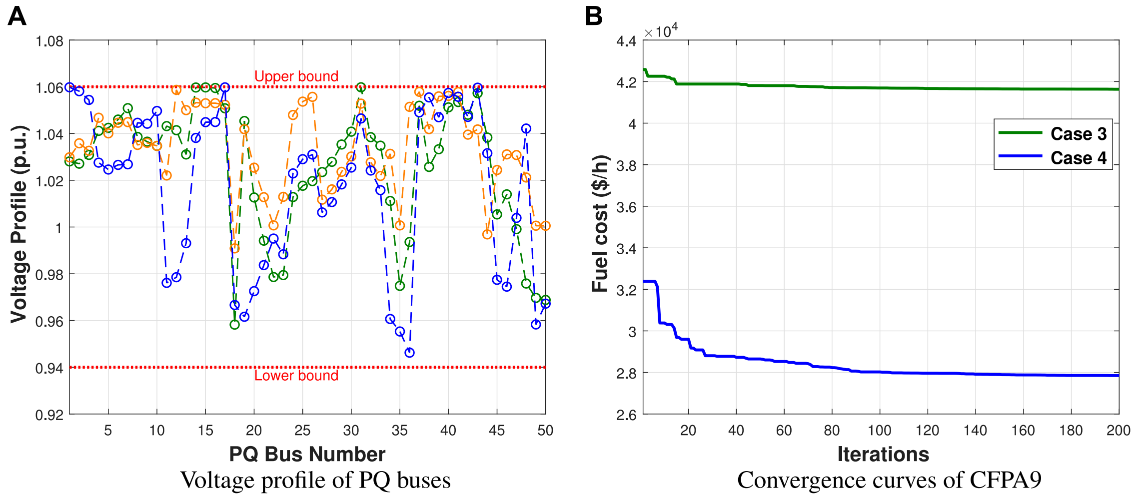

FIGURE 11
Voltage profile and convergence curves of CFPA9 for cases 3 and 4. **(A)** Voltage profile of PQ buses and **(B)** convergence curves of CFPA9.

TABLE 11 Statistical results for case 1 and case 3.

Systems		Min	Mean	Max	SD	*p*_value
IEEE 30-bus	FPA	799.6144	800.3021	801.1084	0.38894	3.0199e-11
	CFPA9	**798.9867**	**799.0729**	**799.2487**	**0.061643**	N/A
IEEE 57-bus	FPA	41666.4325	41724.667	41837.2096	36.9454	3.3384e-11
	CFPA9	**41631.2601**	**41647.5872**	**41666.8326**	**11.8753**	N/A

The bold values indicates the best results.

the stochastic algorithms mentioned above for all benchmark functions except *F*7 and *F*8, where the GOA and ABC outperform CFPA9. The best fitness values of all competitive algorithms have been plotted according to the best run. Moreover, the comparisons of the optimal fitness value done over 30 runs are demonstrated in Figure 6, and it is clear that our approach has a consistent global searching stability and ability.

4.2 Simulation results of optimal power flow

To ensure the quality of the CFPA-based SF with the Sinusoidal map, the optimal power flow issue integrating wind-PV power is investigated. Precisely, the CFPA9 is applied on the two standard benchmark systems, IEEE 30-bus and IEEE 57-bus power systems. All the simulation findings have been implemented for 30 populations, their convergences are examined from the plots obtained of the various objective functions over 200 iterations, and they have been independently run 30 times for each function to perform the statistical analysis.

Besides, the CFPA9 performance is compared with that of the original FPA and those algorithms found in the literature.The considered power systems are examined *via* four case studies defined as follows:

- **Case 1 & 3:** Fuel cost minimization

These cases are calculated according to Equation 16. They reflect the main case, which aims to decrease the cost of fuel only considering power loss, voltage deviation, and emission.

- **Case 2 & 4:** Fuel cost with RES minimization

Equation 18 stands for these test cases; the OPF issue is described with wind-PV power, taking into account the power loss, voltage deviation, and emission.

4.2.1 IEEE 30-bus test system

This power test system possesses 30 buses in which the 1st bus is taken as the slack bus, and there are 6 generators, 4 transformers, 41 lines, and 9 shunt *VAR* compensators. The generators' voltage magnitude bounds are assumed to vary between 0.95$p.u.$ and 1.1$p.u.$ Moreover, the tap ratio transformers are presumed to be in the range of 0.9$p.u.$ to 1.1$p.u.$ The bounds of compensators are taken to be between 0 and 5$p.u.$ The detailed data (line and bus data) for the considered IEEE system are given in (IEEE 30-bus test system data, 1961). Reactive and active powers are given as 126.2$MVAR$ and 283.4MW, respectively. **Figure 7** depicts the considered IEEE 30-bus test system.

Two different cases were considered for this system. As depicted before, case 1 minimizes the total fuel cost only, while the second case reduces the total fuel cost, inserting RESs. The wind power generators have replaced the traditional generators at buses 5 and 11; these wind turbines are the sum of 25 and 20 turbines, respectively. Meanwhile, the generator of bus 13 is changed by a PV generator. The allocation of these RESs into the grid is selected according to the study by (Biswas et al., 2017).

- **Case 1:** Minimization of IEEE 30-bus fuel cost only

All obtained simulation results including control variables of the CFPA9 and FPA algorithms are tabulated in **Table 8**. Thus, according to the best run, **Figure 8** illustrates the convergence curves and distribution runs of the fitness value for case 1. It is clear from this figure that the suggested CFPA9 is superior and converges faster to the optimum than its original algorithm. The fuel cost findings attained in this case for both algorithms, FPA and CFPA9, are 799.6144 ($/h) and **798.9867($/h)**, respectively. In minimizing the cost, the simulation results of power loss, voltage deviation, and emission are **8.5794(MW)**, **0.4969(p.u.)**, and **0.33656(ton/h)**, respectively. Furthermore, the comparison analysis of the outcomes found from all optimization approaches is illustrated in **Table 9**. From that, it is clearly seen that the fuel cost minimum is better than those reported in the literature. According to **Figure 9A**, all load bus voltage profiles obtained from both FPA and CFPA9 are within their specified limits, which means that the feasibility is checked.

- **Case 2:** Minimization of IEEE 30-bus fuel cost with wind and PV

This case aims to optimize the power flow issue by minimizing the total fuel cost that includes the wind-PV cost. **Figure 9B** illustrates the convergence curves of CFPA9 with and without including RESs. The optimal values of control variables are given in **Table 8**. The obtained total fuel cost, emission, voltage deviation, and power loss values are **696.9185($/h)**, **0.1557(ton/h)**, **0.6845(p.u.)**, and **5.9584(MW)**. The cost functions of wind and solar power achieved **173.4157($/h)** and **56.0963($/h)**, respectively. Based on these findings, the value of the fuel cost is reduced by **12.77%** in comparison with the previous case study.

4.2.2 IEEE 57-bus test system

The proposed approach is implemented on the 57-bus test system in this section. The reactive and active power demands of the studied system are 336.4 (MVAR) and 1250.8 (MW), respectively. The line and bus data are taken from (IEEE 57-bus test system data, 1960). This system has seven generating units in which bus 1 is chosen as the slack bus and 80 lines, 50 load buses, three shunt reactive power injections, and 15 transformers. The tap setting for transformers is assumed to vary between 0.9 p. u. and 1.1 p. u. The bounds of voltage magnitude are assumed to be within the range of 0.94–1.06 p. u. The limits of compensators are taken to be between 0 and 20 p. u. Like the first system, the 57-bus test system has been changed by replacing some generators with RESs; two of them are changed by wind generators at buses 2 and 6, and these wind turbines are the sum of 50 and 40 turbines, respectively. Then, bus 9 is considered as the PV generator.

- **Case 3:** Minimization of IEEE 57-bus fuel cost only

For this case study, the attained outcomes are recorded in **Table 10**. **Figure 10** shows a comparison graph of original FPA and the best chaotic FPA on the basis of the best run which consists of the convergence curves and distribution runs. The fuel cost of both algorithms are 41666.432 ($/h) and **41631.2601($/h)**. In addition, the achieved emission, voltage deviation, and power loss values are **1.3858(ton/h)**, **1.6877(p.u.)**, and **13.8706(MW)**, respectively. Furthermore, compared to the outcomes obtained from the newest research studies as illustrated in **Table 9**, the CFPA9 has a lower fitness value. Hence, it should be noted that the simulation findings yielded in this case disclose that the CFPA9 provides better fitness values than other approaches without any violation of any constraint as presented in **Figure 11A**.

- **Case 4:** Minimization of IEEE 57-bus fuel cost with wind-solar

Similar to case 2, CFPA9 has been employed to optimize the optimal power flow issue by minimizing the total fuel cost with the wind and PV generators. Regarding the convergence curves shown in **Figure 11B**, the CFPA9 converges faster to the optimum solution than FPA. According to the best solutions of CFPA9 presented in **Table 9** (case 4), the fuel cost value is **27848.7724(ton/h)**. This fuel cost was reduced by **33.11%** compared to case 3 (without RESs). Moreover, the wind and PV costs are **1411.738(ton/h)** and **1230.2283(ton/h)**, respectively.

To evaluate the performance of the CFPA9, a statistical result was used. Minimum, maximum, mean, standard deviation, and *p*_value of 30 runs' values were calculated as shown in Table 11 and demonstrated the improvement of CFPA9. To this end, it is observed that the attained statistical findings of CFPA9 are close, which means that the outcomes are statistically significant.

5 Conclusion

In this current study, an efficient constrained flower pollination algorithm based on chaos has been suggested and successfully employed to deal with the optimal power flow issue integrating hybrid wind-solar power for case studies involving 30-bus and 57-bus power systems. First, ten different chaotic sequences were employed to enhance the FPA performance. Thus, in view of validating the proposed chaotic algorithms, thirteen benchmark tests are utilized, some of which are multimodal. Accordingly, the obtained results confirm the efficiency and capability of the chaotic FPAs in getting the best solutions, as it outstripped the standard version of the FPA and the well-known approaches ABC, GOA, and DA. Along these lines, these proposed novel chaotic flower pollination algorithms have the ability to handle the various drawbacks of the basic algorithm, in terms of balancing between the exploration and exploitation processes as well as improving the convergence speed. In addition, the overall statistical results proved that the Sinusoidal chaotic map CFPA9 significantly enhances the features of accuracy, reliability, and efficiency in finding the global optimal solution. Second, the best-performing chaotic map, CFPA9, out of the ten chaotic sequences has been recommended to deal with the real-world problem of OPF incorporating wind-PV energy. Furthermore, the outcomes show that CFPA9 with the appropriate constraint handling technique superiority of feasible solution can efficiently improve all objective functions of OPF, which implies that the suggested method is slightly potential and powerful in solving constrained nonlinear complex real-world problems. In accordance with these remarkable outcomes, the authors recommend CFPA with Sinusoidal sequence and SF strategy to handle the OPF issue for a realistic and higher dimension as considered in this present research.

Data availability statement

The original contributions presented in the study are included in the article/Supplementary Material; further inquiries can be directed to the corresponding authors.

Author contributions

All authors listed have made a substantial, direct, and intellectual contribution to the work and approved it for publication.

Conflict of interest

The authors declare that the research was conducted in the absence of any commercial or financial relationships that could be construed as a potential conflict of interest.

Publisher's note

References

Abaci, K., and Yamacli, V. (2016). Differential search algorithm for solving multi-objective optimal power flow problem. *Int. J. Electr. Power and Energy Syst.* 79, 1–10. doi:10.1016/j.ijepes.2015.12.021

Abdel-Basset, M., and Shawky, L. A. (2019). Flower pollination algorithm: A comprehensive review. *Artif. Intell. Rev.* 52 (4), 2533–2557. doi:10.1007/s10462-018-9624-4

Abdullah, A., Enayatifa, R., and Lee, M. (2012). A hybrid genetic algorithm and chaotic function model for image encryption. *AEU - Int. J. Electron. Commun.* 66, 806–816. doi:10.1016/j.aeue.2012.01.015

Abualigah, L., Diabat, A., Mirjalili, S., Abd-Elaziz, M., and Gandomi, A. H. (2021a). The arithmetic optimization algorithm. *Comput. Methods Appl. Mech. Eng.* 376 (2), 113609. doi:10.1016/j.cma.2020.113609

Abualigah, L., Yousri, D., Elaziz, M. A., Ewees, A. A., Al-qaness, A., and Gandomi, A. H. (2021b). Aquila optimizer: A novel meta-heuristic optimization algorithm. *Comput. Industrial Eng.* 157, 107250. doi:10.1016/j.cie.2021.107250

Abualigah, L., Abd Elaziz, M., Sumari, P., Geem, Z., and Amir, H. (2022). Reptile search algorithm (RSA): A nature-inspired meta-heuristic optimizer. *Expert Syst. Appl.* 191, 116158. doi:10.1016/j.eswa.2021.116158

Alasali, F., Nusair, K., Obeidat, A. M., Foudeh, H., and Holderbaum, W. (2021). An analysis of optimal power flow strategies for a power network incorporating stochastic renewable energy resources. *Int. Trans. Electr. Energy Syst.* 31, e13060. doi:10.1002/2050-7038.13060

Alatas, B. (2010). Chaotic bee colony algorithms for global numerical optimization. *Expert Syst. Appl.* 37, 5682–5687. doi:10.1016/j.eswa.2010.02.042

Alhejji, A., Ebeed, M., Kamel, S., and Alyami, S. (2020). Optimal power flow solution with an embedded center-node unified power flow controller using an adaptive grasshopper optimization algorithm. *IEEE Access* 99, 119020–119037. doi:10.1109/ACCESS.2020.2993762

Arora, S., and Singh, S. (2017). An improved butterfly optimization algorithm with chaos. *J. Intell. Fuzzy Syst.* 32, 1079–1088. doi:10.3233/JIFS-16798

Basturk, B., and Karaboga, D. (2006). "An artificial bee colony (ABC) algorithm for numeric function optimization," in Proceedings of the IEEE Swarm Intelligence Symposium (Indianapolis: USA), 4–12.

Bentouati, B., Chettih, S., and Chaib, L. (2017). Interior search algorithm for optimal power flow with non-smooth cost functions. *Cogent Eng.* 4, 1292598–1292617. doi:10.1080/23311916.2017.1292598

Biswas, P., Suganthan, P., and Amaratunga, G. (2017). Optimal power flow solutions incorporating stochastic wind and solar power. *Energy Convers. Manag.* 148, 1194–1207. doi:10.1016/j.enconman.2017.06.071

Biswas, P. P., Suganthan, P., Mallipeddi, R., and Amaratunga, G. A. (2018a). Optimal power flow solutions using differential evolution algorithm integrated with effective constraint handling techniques. *Eng. Appl. Artif. Intell.* 68, 81–100. doi:10.1016/j.engappai.2017.10.019

Biswas, P. P., Suganthan, P. N., Qu, B. Y., and Amaratunga, G. A. (2018b). Multiobjective economic-environmental power dispatch with stochastic wind-solar-small hydro power. *Energy* 150 (5), 1039–1057. doi:10.1016/j.energy.2018.03.002

Bonab, S. M. M., Rabiee, A., and Ivatloo, B. (2016). Voltage stability constrained multi-objective optimal reactive power dispatch under load and wind power uncertainties: A stochastic approach. *Renew. Energy* 85, 598–609. doi:10.1016/j.renene.2015.07.021

Bouchekara, H. R. E. H., Chaib, A. E., and Abido, M. A. (2016a). Multi-objective optimal power flow using a fuzzy based grenade explosion method. *Energy Syst.* 7, 699–721. doi:10.1007/s12667-016-0206-8

Bouchekara, H. R. E. H., Chaib, A. E., Abido, M. A., and El-Sehiemy, R. A. (2016b). Optimal power flow using an improved colliding bodies optimization algorithm. *Appl. Soft Comput.* 42, 119–131. doi:10.1016/j.asoc.2016.01.041

Bouchekara, H. R. E. H., Abido, M. A., and Chaib, A. E. (2016c). Optimal power flow using an improved electromagnetism-like mechanism method. *Electr. Power Components Syst.* 44 (4), 434–449. doi:10.1080/15325008.2015.1115919

Cai, J. J., Ma, X. Q., Li, X., Yang, Y., Peng, H., and Wang, X. (2007). Chaotic ant swarm optimization to economic dispatch. *Electr. Power Syst. Res.* 77, 1373–1380. doi:10.1016/j.epsr.2006.10.006

Chaib, A. E., Bouchekara, H. R. E. H., Mehasni, R., and Abido, M. A. (2016). Optimal power flow with emission and non-smooth cost functions using backtracking search optimization algorithm. *Int. J. Electr. Power & Energy Syst.* 81, 64–77. doi:10.1016/j.ijepes.2016.02.004

Chang, T. (2010). Investigation on frequency distribution of global radiation using different probability density functions. *Intern. J. Appl. Sci. Eng.* 8 (2), 99–107. doi:10.6703/IJASE.2010.8(2).99

Daqaq, F., Ouassaid, M., and Ellaia, R. (2021). A new meta-heuristic programming for multi-objective optimal power flow. *Electr. Eng.* 103, 1217–1237. doi:10.1007/s00202-020-01173-6

Daqaq, F., Ellaia, R., Ouassaid, M., Zawbaa, M. H., and Kamel, S. (2022). Enhanced chaotic manta ray foraging algorithm for function optimization and optimal wind farm layout problem. *IEEE Access* 10, 78345–78369. doi:10.1109/ACCESS.2022.3193233

Deb, K. (2000). An efficient constraint handling method for genetic algorithms. *Comput. Methods Appl. Mech. Eng.* 186 (2), 311–338. doi:10.1016/s0045-7825(99)00389-8

Derrac, J., Garcia, S., Molina, D., and Herrera, F. (2011). A practical tutorial on the use of nonparametric statistical tests as a methodology for comparing evolutionary and swarm intelligence algorithms. *Swarm Evol. Comput.* 1, 3–18. doi:10.1016/j.swevo.2011.02.002

Duman, S. (2017). Symbiotic organisms search algorithm for optimal power flow problem based on valve-point effect and prohibited zones. *Neural comput. Appl.* 28, 3571–3585. doi:10.1007/s00521-016-2265-0

Elattar, E., and ElSayed, S. K. (2019). Modified JAYA algorithm for optimal power flow incorporating renewable energy sources considering the cost, emission, power loss and voltage profile improvement. *Energy* 178, 598–609. doi:10.1016/j.energy.2019.04.159

Elattar, E. E. (2019). Optimal power flow of a power system incorporating stochastic wind power based on modified moth swarm algorithm. *IEEE Access* 7, 89581–89593. doi:10.1109/access.2019.2927193

El-Fergany, A. A., and Hasanien, H. M. (2018). Tree-seed algorithm for solving optimal power flow problem in large-scale power systems incorporating validations and comparisons. *Appl. Soft Comput.* 64, 307–316. doi:10.1016/j.asoc.2017.12.026

El-Sattar, S. A., Kamel, S., el Sehiemy, R. A., Jurado, F., and Yu, J. (2019). Single and multi-objective optimal power flow frameworks using Jaya optimization technique. *Neural comput. Appl* 31, 8787–8806. doi:10.1007/s00521-019-04194-w

Essam, H. H., Mohammed, R. S., Fatma, A. H., Hassan, S., and Hassaballah, M. (2020). Lévy flight distribution: A new metaheuristic algorithm for solving engineering optimization problems. *Eng. Appl. Artif. Intell.* 94, 103731. doi:10.1016/j.engappai.2020.103731

Gandomi, A., Yang, X. S., Talatahari, S., and Alavi, A. (2013). Firefly algorithm with chaos. *Commun. Nonlinear Sci. Numer. Simul.* 18, 89–98. doi:10.1016/j.cnsns.2012.06.009

Ghafil, H. N., and Jármai, K. (2020). Dynamic differential annealed optimization: New metaheuristic optimization algorithm for engineering applications. *Appl. Soft Comput.* 93, 106392. doi:10.1016/j.asoc.2020.106392

Hashim, F. A., Houssein, E. H., Mabrouk, M. S., Al-Atabany, W., and Mirjalili, S. (2019). Henry gas solubility optimization: A novel physics-based algorithm. *Future Gener. Comput. Syst.* 101, 646–667. doi:10.1016/j.future.2019.07.015

Hashim, F. A., Houssein, E. H., Hussain, K., Mabrouk, M. S., and Al-Atabany, W. (2022). Honey badger algorithm: New metaheuristic algorithm for solving optimization problems. *Math. Comput. Simul.* 192, 84–110. doi:10.1016/j.matcom.2021.08.013

Hayyolalam, V., and Pourhaji, K. A. A. (2020). Black Widow optimization algorithm: A novel meta-heuristic approach for solving engineering optimization problems. *Eng. Appl. Artif. Intell.* 87, 103249. doi:10.1016/j.engappai.2019.103249

He, Y. Y., Zhou, J. Z., Zhou, X. Q., Chen, H., and Qin, H. (2009). Comparison of different chaotic maps in particle swarm optimization algorithm for long term cascaded hydroelectric system scheduling. *Chaos Solit. Fractals* 42, 3169–3176. doi:10.1016/j.chaos.2009.04.019

Heidari, A. A., Abbaspour, R. A., and Jordehi, A. R. (2017). An efficient chaotic water cycle algorithm for optimization tasks. *Neural comput. Appl.* 28, 57–85. doi:10.1007/s00521-015-2037-2

Heidari, A. A., Mirjalili, S., Faris, H., Aljarah, I., Mafarja, M. M., and Chen, H. (2019). Harris hawks optimization: Algorithm and applications. *Future Gener. Comput. Syst.* 97, 849–872. doi:10.1016/j.future.2019.02.028

Holland, J. (1975). *Adaptation in natural and artificial systems*. Ann Arbor, MI, USA: University of Michigan Press.

Houssein, E. H., Hassan, M. H., Mahdy, M. A., and Kamel, S. (2022). Development and application of equilibrium optimizer for optimal power flow calculation of power system. *Appl. Intell.* 1–22. doi:10.1007/s10489-022-03796-7

IEEE 57-bus test system data (1960). Power systems test case archive. Available from: http://labs.ece.uw.edu/pstca/pf57/pg_tca57bus.htm.

IEEE 30-bus test system data (1961). Power systems test case archive. Available from: http://labs.ece.uw.edu/pstca/pf30/pg_tca30bus.htm.

Jia, D., Zheng, G., and Khan, M. K. (2011). An effective memetic differential evolution algorithm based on chaotic local search. *Inf. Sci. (N. Y).* 181, 3175–3187. doi:10.1016/j.ins.2011.03.018

Jordehi, A. R. (2014). A chaotic-based big bang-big crunch algorithm for solving global optimization problems. *Neural comput. Appl.* 25, 1329–1335. doi:10.1007/s00521-014-1613-1

Jordehi, A. R. (2015). A chaotic artificial immune system optimisation algorithm for solving global continuous optimisation problems. *Neural comput. Appl.* 26, 827–833. doi:10.1007/s00521-014-1751-5

Kennedy, J., and Eberhart, R. C. (1995). "Particle swarm optimization," in Proceedings of the IEEE international conference on neural networks (Piscataway, NJ, USA, 1942–1948.

Kirkpatrick, S., Gelatt, C. D., and Vecchi, M. P. (1983). Optimization by simulated annealing. *Science* 220 (4598), 671–680. doi:10.1126/science.220.4598.671

Letellier, C. (2019). *Chaos in nature*. 2nd edn. Singapore: World Scientific.

Meng, A., Zeng, C., Wang, P., Zhou, T., and Zheng, X. (2021). A high-performance crisscross search based grey wolf optimizer for solving optimal power flow problem. *Energy* 225, 120211. doi:10.1016/j.energy.2021.120211

Mirjalili, S., Lewis, A., and Mirjalili, S. M. (2014). Adaptive gbest-guided gravitational search algorithm. *Neural comput. Appl.* 25, 1569–1584. doi:10.1007/s00521-014-1640-y

Mirjalili, S., Gandomi, A. H., Mirjalili, S. Z., Saremi, S., Faris, H., and Mirjalili, S. M. (2017). Salp swarm algorithm: A bio-inspired optimizer for engineering design problems. *Adv. Eng. Softw.* 114, 163–191. doi:10.1016/j.advengsoft.2017.07.002

Mirjalili, S. S. C. A. (2016). Sca: A sine cosine algorithm for solving optimization problems. *Knowl. Based. Syst.* 96, 120–133. doi:10.1016/j.knosys.2015.12.022

Mohamed, A. A. A., Mohamed, Y. S., El-Gaafary, A. A., and Hemeida, A. M. (2017). Optimal power flow using moth swarm algorithm. *Electr. Power Syst. Res.* 142, 190–206. doi:10.1016/j.epsr.2016.09.025

Morshed, M. J., Hmida, J. B., and Fekih, A. (2018). A probabilistic multi-objective approach for power flow optimization in hybrid wind-PV-PEV systems. *Appl. Energy* 211, 1136–1149. doi:10.1016/j.apenergy.2017.11.101

Mugemanyi, S., Qu, Z., Rugema, F. X., Dong, Y., Bananeza, C., and Wang, L. (2020). Optimal reactive power dispatch using chaotic bat algorithm. *IEEE Access* 8, 65830–65867. doi:10.1109/ACCESS.2020.2982988

Nguyen, T. T. (2019). A high performance social spider optimization algorithm for optimal power flow solution with single objective optimization. *Energy* 171, 218–240. doi:10.1016/j.energy.2019.01.021

Niu, P., Li, J., Chang, L., Zhang, X., Wang, R., and Li, G. (2019). A novel flower pollination algorithm for modeling the boiler thermal efficiency. *Neural process. Lett.* 49, 737–759. doi:10.1007/s11063-018-9854-0

Pavlyukevich, I. (2007). Lévy flights, non-local search and simulated annealing. *J. Comput. Phys.* 226, 1830–1844. doi:10.1016/j.jcp.2007.06.008

Priya, K., and Rajasekar, N. (2019). Application of flower pollination algorithm for enhanced proton exchange membrane fuel cell modelling. *Int. J. Hydrogen Energy* 44 (33), 18438–18449. doi:10.1016/j.ijhydene.2019.05.022

Rodrigues, D., De Rosa, G. H., Passos, L. A., and Papa, J. P. (2020). "Adaptive improved flower pollination algorithm for global optimization," in *Nature-inspired computation in data mining and machine learning* (Springer), 1–21.

Samy, M., Barakat, S., and Ramadan, H. (2019). A flower pollination optimization algorithm for an off-grid pv-fuel cell hybrid renewable system. *Int. J. hydrogen energy* 44, 2141–2152. doi:10.1016/j.ijhydene.2018.05.127

Saremi, S., Mirjalili, S., and Lewis, A. (2014). Biogeography-based optimisation with chaos. *Neural comput. Appl.* 25, 1077–1097. doi:10.1007/s00521-014-1597-x

Sayed, G. I., Hassanien, A. E., and Azar, A. T. (2017). Feature selection via a novel chaotic crow search algorithm. *Neural comput. Appl.* 31, 171–188. doi:10.1007/s00521-017-2988-6

Shambour, M. K. Y., Abusnaina, A. A., and Alsalibi, A. I. (2019). Modified global flower pollination algorithm and its application for optimization problems. *Interdiscip. Sci. Comput. Life Sci.* 11, 496–507. doi:10.1007/s12539-018-0295-2

Shilaja, C., and Arunprasath, T. (2019). Optimal power flow using moth swarm algorithm with gravitational search algorithm considering wind power. *Future Gener. Comput. Syst.* 98, 708–715. doi:10.1016/j.future.2018.12.046

Singh, A. P., and Kaur, A. (2019). Flower pollination algorithm for feature analysis of kyoto 2006+ data set. *J. Inf. Optim. Sci.* 40 (2), 467–478. doi:10.1080/02522667.2019.1580886

Sulaiman, M. H., Mustaffa, Z., Mohamad, A. J., Saari, M. M., and Mohamed, M. R. (2021). Optimal power flow with stochastic solar power using barnacles mating optimizer. *Int. Trans. Electr. Energy Syst.* 31, e12858. doi:10.1002/2050-7038.12858

Taher, M. A., Kamel, S., Jurado, F., and Ebeed, M. (2019a). An improved moth-flame optimization algorithm for solving optimal power flow problem. *Int. Trans. Electr. Energy Syst.* 29, e2743. doi:10.1002/etep.2743

Taher, M. A., Kamel, S., Jurado, F., and Ebeed, M. (2019b). Optimal power flow solution incorporating a simplified UPFC model using lightning attachment procedure optimization. *Int. Trans. Electr. Energy Syst.* 30, e12170. doi:10.1002/2050-7038.12170

Tong, H., Zhu, Y., Pierezan, J., Xu, Y., and Coelho, L. d. S. (2022). Chaotic Coyote optimization algorithm. *J. Ambient. Intell. Humaniz. Comput.* 13 (1), 2807–2827. doi:10.1007/s12652-021-03234-5

Too, J., and Abdullah, A. R. (2020). Chaotic atom search optimization for feature selection. *Arab. J. Sci. Eng.* 45 (8), 6063–6079. doi:10.1007/s13369-020-04486-7

Trivedi, I. N., Jangir, P., and Parmar, S. A. (2016). Optimal power flow with enhancement of voltage stability and reduction of power loss using ant-lion optimizer. *Cogent Eng.* 3, 1208942. doi:10.1080/23311916.2016.1208942

Vaccaro, A., and Cañizares, C. A. (2018). A knowledge-based framework for power flow and optimal power flow analyses. *IEEE Trans. Smart Grid* 9, 230–239. doi:10.1109/PESGM.2017.8273989

Vasant, P. M. (2012). Meta-heuristics optimization algorithms in engineering business, economics, and finance. *IGI Glob.* doi:10.4018/978-1-4666-2086-5

Wang, Z., Xie, H., He, D., and Chan, S. (2019a). Wireless sensor network deployment optimization based on two flower pollination algorithms. *IEEE Access* 7, 180590–180608. doi:10.1109/access.2019.2959949

Wang, K., Li, X., and Gao, L. (2019b). A multi-objective discrete flower pollination algorithm for stochastic two-sided partial disassembly line balancing problem. *Comput. Industrial Eng.* 130, 634–649. doi:10.1016/j.cie.2019.03.017

Wanga, G., Guo, L., Gandomi, A., Hao, G., and Wangb, H. (2014). Chaotic krill herd algorithm. *Inf. Sci. (N. Y).* 274, 17–34. doi:10.1016/j.ins.2014.02.123

Warid, W. (2020). Optimal power flow using the AMTPG-jaya algorithm. *Appl. Soft Comput.* 91, 106252. doi:10.1016/j.asoc.2020.106252

Wilcoxon, F. (1945). Individual comparisons by ranking methods. *Biom. Bull.* 1, 80–83. doi:10.2307/3001968

Wolpert, D. H., and Macready, W. G. (1997). No free lunch theorems for optimization. *IEEE Trans. Evol. Comput.* 1, 67–82. doi:10.1109/4235.585893

Xie, Z. Q., Ji, T. Y., Li, M. S., and Wu, Q. H. (2018). Quasi-Monte Carlo based probabilistic optimal power flow considering the correlation of wind speeds using copula function. *IEEE Trans. Power Syst.* 33, 2239–2247. doi:10.1109/tpwrs.2017.2737580

Yang, X. S. (2010). *Engineering optimization: An introduction with metaheuristic applications*. New Jersey: John Wiley & Sons. doi:10.1002/9780470640425

Yang, X. S. (2012). Flower pollination algorithm for global optimization. *Int. Conf. Unconv. Comput. Nat. Comput.*, 240–249. doi:10.1007/978-3-642-32894-7_27

Yang, X. S. (2014). *Nature-inspired optimization algorithms*. 1st edn. London.

Yessef, M., Bossoufi, B., Taoussi, M., and Lagrioui, A. (2022a). Enhancement of the direct power control by using backstepping approach for a doubly fed induction generator. *Wind Eng.* 46 (5), 1511–1525. doi:10.1177/0309524X221085670

Yessef, M., Bossoufi, B., Taoussi, M., Lagrioui, A., and Chojaa, H. (2022b). Overview of control strategies for wind turbines: ANNC, FLC, SMC, BSC, and PI controllers. *Wind Eng.* [Epub ahead of print 28 June 2022]. doi:10.1177/0309524X221109512

Yuan, X., Zhang, B., Wang, P., Liang, J., Yuan, Y., Huang, Y., et al. (2017). Multi-objective optimal power flow based on improved strength Pareto evolutionary algorithm. *Energy* 122, 70–82. doi:10.1016/j.energy.2017.01.071

Zamani, H., Mohammad, H., and Gandomi, A. H. (2022). Starling murmuration optimizer: A novel bio-inspired algorithm for global and engineering optimization. *Comput. Methods Appl. Mech. Eng.* 392, 114616. doi:10.1016/j.cma.2022.114616

Zhao, W., Zhang, Z., and Wang, L. (2020). Manta ray foraging optimization: An effective bio-inspired optimizer for engineering applications. *Eng. Appl. Artif. Intell.* 87, 103300. doi:10.1016/j.engappai.2019.103300